2014

Synthesis of H-branch alkanes

Wilde, M.

Wilde, M. (2014) 'Synthesis of H-branch alkanes', The Plymouth Student Scientist, 7(1), p. 50-99.
http://hdl.handle.net/10026.1/14052

The Plymouth Student Scientist
University of Plymouth

Synthesis of H-branch alkanes

Michael Wilde

Project Advisor: C. Anthony Lewis, School of Geography, Earth and Environmental Sciences, Plymouth University, Drake Circus, Plymouth, PL4 8AA

Abstract

The complex composition of petroleum and the chromatographic challenge it presents has led to its study becoming a key field in contemporary scientific research. Rising concerns over the impact of petroleum within the environment have spurred the need to fingerprint and identify individual oils in order to understand its fate within the environment.

The complexity of petroleum lies solely in its origins and thermal processes it undergoes during formation, resulting in it containing hundreds of thousands of different, unknown organic compounds. The majority of petroleum is observed in GC analysis as a 'hump' of unresolvable peaks; this characteristic hump is known as the Unresolved Complex Mixture or UCM. There have been several advances in the separation of oil e.g. GC×GC-MS, dedicated to resolving and identifying compounds within the UCM that could be potential toxicological hazards within the environment.

This has led to the unique method of synthesising model UCMs and the possible compounds believed to be within petroleum. Previous investigations, involving the synthesis of C_{19} T-branch alkanes have provided evidence to suggest that such structures are present within the aliphatic fraction of some UCMs. This has led onto the synthesis of C_{19} H-branch alkanes for the purpose of identifying them within the aliphatic UCM and studying the chromatographic effect of branching within alkanes.

A C_{19} H-branch alkane was successfully synthesised following the improvement of a Grignard reaction, producing a 3° alcohol which was subsequently dehydrated and hydrogenated to give the desired 5,7-substituted alkane. Comprehensive analysis was performed throughout the investigation, utilising FT-IR, GC-FID and GC-MS, to identify the products of the reactions and confirm the final structure of the desired H-branch alkane.

The retention index for the completed H-branch subdivision was calculated and compared with previously studied H- and T-branch alkanes along with pristane; prior to this investigation commonly known to be the earliest eluting C_{19} alkane. As a result of this study, two of the H-branch alkanes are now known to have retention indices of 1688 and 1692 Kovats, being lower than n-heptadecane and pristane at 1707 Kovats, making them some of the earliest eluting C_{19} branched alkanes.

1. Introduction

1.1 Overview

The aim of the investigation was to explore the synthesis of a H-branch alkane and the potential applications of synthetic hydrocarbons to help resolve the complex composition of petroleum. Despite the routine use of petroleum as a major, important energy source, the knowledge of its complex composition and its chemical properties is relatively small yet vital if the use of petroleum is to be optimised (Gough and Rowland, 1990). Understanding the diverse make-up of petroleum could enhance the discovery, refining, environmental effects and characterisation of oil (Gough and Rowland, 1990). A unique approach to gain an insight into the complex composition is to create synthetic mixtures of already identified fractions within petroleum and biodegraded petroleum such as aliphatic, aromatic, asphaltenic and naphthenic hydrocarbons. The synthetic route to obtain a desired hydrocarbon involves the exploration of carbon-carbon bond forming reactions and deciding the correct strategy to adopt. This research involved considering several synthetic pathways but the experimental research focused on organometallic reactions.

1.2 Crude Oil and the UCM

Crude oil is a complex mixture, primarily consisting of hydrocarbons with low quantities of NSO compounds and trace amounts of metals such as nickel and vanadium (Killops and Killops, 2005). The main hydrocarbon mixture can be subcategorised into acyclic alkanes or paraffins, cycloalkanes or naphthenes and aromatic compounds (Killops and Killops, 2005). The composition of an oil is related to the kerogen from which it was generated.

The generation of crude oil stems back from the sedimentation of organic matter from decaying bacteria, plants and algae within the water column. As the layering of sediment increases, the organic matter becomes embedded in sedimentary rock experiencing bacterial decay producing humic acids. Within the sedimentary rock, the organic compounds undergo further chemical processes such as microbial degradation and oxidation which breaks down the matter into kerogen and bitumen, a process known as diagenesis (Engel and Macko, 1993). Bitumen is the fraction of kerogen soluble in organic solvents (Miles, 1989).

When the kerogen encounters additional burial with increased temperature and pressure, it undergoes thermal change which results in the release of hydrocarbon liquids and gases, a phenomenon called catagenesis (Killops and Killops, 2005). This process involves thermal degradation and cracking, producing crude oil. The crude oil is able to migrate up through the permeable rock and collect in small pore within the rock from which it can be drilled, refined and used as an energy source. The long maturation and accumulation of crude oil demonstrates how the crude oil composition depends on the environment and conditions from which it was produced, resulting in each crude oil having a complex identity.

Chromatography reveals the complexity of crude oil, seen by its incomplete separation resulting in a group of unresolved peaks or a ‘hump’. The mixture of hydrocarbons responsible for this hump in the chromatogram is known as the unresolved complex mixture or UCM. The extent of the UCM and resolvable peaks varies between petroleum samples but a more pronounced UCM, seen as a larger indistinguishable hump, is characteristic of weathered oils. Conversely, unweathered

oils often show little or no UCM with a series of distinguishable, resolved peaks corresponding to long chain aliphatic alkanes.

When oil is exposed to the environment, particularly marine environments during oil tanker spills, it experiences weathering which involves processes such as photodegradation, biodegradation, oxidation and dissolution. Weathering results in chemical alterations of hydrocarbons, changing the composition of the oil. Certain hydrocarbons are susceptible to biodegradation and the products of biodegradation can produce characteristic biomarkers indicative of the original compounds (Killops and Killops, 2005).

Aside from weathering, the refinery process of oil can also contribute to an increased UCM. For example, visbreaking involves cracking the heavy distillate fractions into lighter more usable fractions such as petrol (gasoline) (Wauquier, 1995). However, a heavy residue is also produced which contains thermally altered and unresolvable compounds. After distillation, this residue is blended back into the fuel and the thermally altered structures produced will increase the 'hump' (Wauquier, 1995).

Identifying the compounds in the UCM of weathered or refined oils, can help determine the origin of the oils and as a result be used to assign responsibility and ownership to companies when oil is spilt, stolen and transported.

1.3 Chromatographic Techniques and Applications

The identification of compounds within the UCM has many potential applications however the process relies on the successful separation of complex mixtures with highly resolved results, which may be achieved by developing chromatographic techniques. The separation of crude oil constituents incorporates a variety of chromatographic techniques often coupled together, ranging from thin-layer and column chromatography, GC and HPLC to advanced GC×GC with sensitive detectors such as FID and MS.

Frysinger *et al.* (2003) completed a comprehensive separation scheme to determine the different fractions of hydrocarbons within the UCM of petroleum-contaminated sediments and were successful in identifying individual alkanes and cycloalkanes in the aliphatic fraction. Prior to analysis with GC-MS, they completed two separations using column chromatography, separating the polar and non-polar compounds. The first column chromatographic separation involved a silica gel column, collecting two fractions with hexane and a hexane:dichloromethane (1:1 v/v) mixture. The two fractions were then further separated using silver-impregnated silica gel, producing four fractions; saturates, one ring, two ring and three ring aromatics (Frysinger *et al.*, 2003).

After fractioning the UCM, Frysinger *et al.* (2003) analysed the isolated portions by GC-MS and GC×GC-FID. The two dimensional gas chromatography involved using a non-polar volatility selective column coupled with a polarity selective column to resolve naphthalene compounds, later replaced with a shape selective column to resolve branched alkanes and cycloalkanes (Frysinger *et al.*, 2003). The GC×GC was successful in determining the presence of three-carbon-substituted naphthalene isomers and two methylphenanthrene isomers; the abundance of the different isomers varied from the typical distributions found in petroleum fuels, characteristic to the type of weathering different oils experienced. The GC-MS analysis enabled

the identification of isoprenoid biomarkers, such as pristane and phytane and isomeric alkyl cycloalkanes (Frysinger *et al.*, 2003).

Identifying oil by utilising the unique information given by the analysis of the UCM is known as 'fingerprinting'. Biomarkers are parts of biological molecules present in oil; during diagenesis and catagenesis, the complex hydrocarbons in organic matter break down and the remaining skeletal structures, resistant to further biodegradation reside in the UCM (Wang and Stout, 2007). The biomarkers give an indication of the environment from which the oil was derived. For example, if dinosterane was identified (Figure 1), the biodegraded form of dinosterol produced by a marine organism dinoflagellate would indicate the oil is derived from marine organic matter, and as dinosteranes have not been found in oils before the Triassic age, this would age the oil up to 250 million years old (Wang and Stout, 2007, Summons *et al.*, 1992). The information obtained from the marine biomarker can be useful when comparing spilt foreign oils which contain high concentrations of plant biomarkers not local to marine sediments.

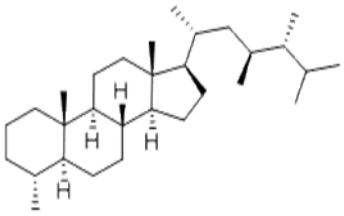

Figure 1: Structure of dinosterane (Guidechem, 2012)

Burns *et al.* (2004) monitored the flux of organic carbon matter along the shelf of the Gulf of Papua. Their samples contained large UCMs which showed the presence of petroleum in the environment. They used $AgNO_3$ impregnated silica gel column chromatography to purify the *n*-alkane hydrocarbons and used GC-FID and GC-MS to identify the structures of several biomarkers such as $C_{27\text{-}33}$ hopanes and $C_{27\text{-}29}$ steranes (Burns *et al.*, 2004).

The *n*-alkane fraction, isolated by Burns *et al.* (2004) was considered too 'waxy' to originate from lubricating oil from anthropogenic sources and too weathered to be contamination from the fuel of the sampling ship used to deploy and collect the sediment traps. Lubricating oils are usually dewaxed when processed (Albaigés *et al.*, 1983). The hopane and sterane biomarkers found, corresponded to marine carbonate sourced oil which is local to the Gulf of Papua environment from natural seepage of oil (Burns *et al.*, 2004). Highly branched isoprenoids (HBIs), characteristic of diatoms and phytoplankton were also resolved by MRM-GC-MS (Multiple Reaction Monitoring), found in the sediment trap samples, indicative of oil from marine origins (Belt *et al.*, 2000).

McCaffery *et al.* (2009) investigated oil-contaminated soils of a crude oil processing facility to determine if the oil present was due to natural crude oil seepage (NCS) from offshore deposits or from anthropogenic petroleum (APH) as a subsequent result of previous leaks at the facility. They expected a more developed, complex

UCM for NCS sources due to increased weathering. The oil samples were analysed by an isotope-ratio mass spectrometer and GC-MS (McCaffery *et al.*, 2009).

Three of the five sites sampled by McCaffery *et al.* (2009) within the facility, contained oil from NCS and had distinctly weathered *n*-alkane UCM fractions; with a low maximum retention time of 50min, compared with the sites contaminated by APH oil; with higher maximum retention time of 70min. The biodegraded NCS crude oil was identified by the typically high concentration of tricyclic terpanes and C_{27}-diasteranes, the petroleum processed at the facility were different; containing higher abundances of C_{28}-ergosteranes (McCaffery *et al.*, 2009). The different levels of PAHs highlight the dissimilar degradation experienced by both oils. Other biomarker ratios such as pristane: phytane were not conclusive or influential in the determination of petroleum sources (McCaffery *et al.*, 2009). This inadequacy of otherwise standard reference compounds in some situations emphasises the need for more research into other characteristic isotopic ratios and biomarkers, to account for the considerable variation displayed in the UCM.

In 1989, the Exxon Valdez tanker struck the Bligh reef in Prince William Sound, Alaska, resulting in 258,000 barrels or 11 million US gallons of Alaska North Slope crude oil to be released into the marine environment of the Gulf of Alaska (Wells *et al.*, 1995). The local sediments and marine organisms were investigated by GC-MS to distinguish between the background petroleum hydrocarbons and the crude oil released by the spill in order to monitor the extent of pollution. A method with a solo application of fingerprinting Exxon Valdez crude oil was proposed, based on the PAH concentrations within the UCM and with additional support from the saturate fraction when possible (Wells *et al.*, 1995). The PAH fraction of processed and refined petroleum, predominantly consists of light PAHs such as naphthalenes and phenanthrenes which have low carbon numbers and molecular masses with increased water solubility (Wells *et al.*, 1995). Therefore, weathered crude oil from the spill was characterised by the removal of many light PAHs from the sample which had dissolved and been washed from the UCM. The depletion of soluble compounds leaves a higher concentration of insoluble PAHs such as chrysenes; the ratio of alkylated chrysenes relative to alkylated phenanthrenes was significant in fingerprinting Exxon Valdez crude oil (Wells *et al.*, 1995). Boehm et al. (1997) show the gradual degradation of Exxon Valdez crude oil and its distinct fingerprint, the saturated fraction displaying the formation of a typical UCM hump.

Mansuy *et al.* (1997) investigated the use of GC-IRMS, gas chromatography coupled with an isotope-ratio mass spectrometer, as a supporting method to GC and GC-MS in the identification of *n*-alkanes in weathered oil. GC-IRMS was used to measure the isotopic composition of weathered oil and whether biodegraded alterations affect the resemblance of the oil to its non-degraded fresh oil. The results showed that weathering does not affect the isotopic composition of identifiable compounds; components still resolvable after weathering (Mansuy *et al.*, 1997). However, in the absence of resolvable *n*-alkanes e.g. in severely weathered oil, and without the identification of biomarker ratios using GC-MS, the results of GC-IRMS alone does not provide irrefutable evidence to relate degraded oils back to their original sources. Conversely, as a support technique in the analysis of oils with similar overall carbon isotopic ratios, GC-IRMS can provide detailed isotopic information for individual compounds; adding another level of resolution (Mansuy *et al.*, 1997).

The potential role of the *n*-alkane fraction in the characterising the UCM was highlighted by Gough *et al.* (1997). They hypothesised that the precursor compounds of straight chain components in weathered petroleum such as straight monocarboxylic acids, possible products of microbial degradation on aliphatic hydrocarbons, were partially comprised of monoalkyl-substituted T-branch alkanes (Gough and Rowland, 1990, Gough *et al.*, 1992). A synthetic, aliphatic model UCM of T-branch alkanes was biodegraded alongside an extracted UCM from a lubricating base oil, revealing comparative rates of degradation; the results support the idea of such alkanes are present in the UCM (Gough and Rowland, 1990).

Despite GC×GC-FID providing adequate separation for Frysinger *et al.* (2003) who identified individual hydrocarbon groups such as an isomeric mixture of napthalenes in contaminated sediments, analysis by the same technique of motor oils before entering the environment was not sufficient (Mao *et al.*, 2009). Motor oils consist of mineral base oils with additional wear-agents and additives, the successful classification of hydrocarbons and their distributions would provide a detailed insight into the degradability, physico-chemical and performance properties of the oil (Mao *et al.*, 2009). In order to improve previous GC-MS and GC×GC analysis, Mao *et al.* (2009) introduced a prefractionation step, coupling HPLC with two-dimensional gas chromatography.

Direct comparison of GC×GC and HPLC-GC×GC chromatograms showed the improved technique was far superior; the complete separation of the saturated and aromatic fractions resulted in the clear separation of cycloalkanes and resolution of individual ring numbers (Mao *et al.*, 2009). Identification of the cycloalkanes by GC×GC-TOF-MS revealed the structures of biomarkers such as hopanes, indicative of motor oil pollution (Mao *et al.*, 2009, McCaffery *et al.*, 2009). Determining the accurate distributions of resolvable fractions, e.g. 82% saturate comprised of 32% cycloalkanes and in total 18% aromatic, allowed for the quantitative determination of non-chromatographic resins and additives (Mao *et al.*, 2009). The difference in additive amounts was believed to be directly related to the performance properties of the oil.

The investigation of Mao *et al.* (2009) incorporated the analysis of synthetic oil; the hydrocarbon distribution was dominated by saturated alkanes with a much less smaller contribution from cycloalkanes and aromatic compounds. The difference between the synthetic oil and mineral based oils may be due to cracking during production processes and as a result Mao *et al.* (2009) suggest the synthetic oil may be more resistant to oxidation processes. Therefore synthetic oil may have different toxicity and effects within the environment, making this a potential area of further related study.

1.4 Advanced Techniques and Future Research

The conventional techniques, using GC and GC-MS, provided sufficient separation to begin characterising a few key components within the UCM, sparking an interest in the composition of crude oils and highlighted the UCM as a potential toxic hazard for organisms within the environment. Smith *et al.* (2001) measured the toxicity of monoaromatic compounds identified in the UCM using GC-MS. The results showed that an accumulation of these compounds and UCMs within the mussels *Mytilus edulis*, decreases the feeding rate by more than 60% (Smith *et al.*, 2001). However to gain a greater, detailed understanding of the UCM and advance the fingerprinting

of petroleum, further innovation in separation techniques and instrumentation with high resolving power is required.

Booth *et al.* (2007) utilised the exceptional chromatographic resolution of two-dimensional gas chromatography coupled with time-of-flight mass spectrometry (GC×GC-TOF-MS) to analysis the aromatic fraction extracted from UCMs within mussel tissue. The overall result showed the successful separation of over 3400 different aromatic compounds (Booth *et al.*, 2006).

The diminishing reserves of crude oil and its high demand as an energy source has led to the development of different ways to harvest the resource, such as extracting the petroleum from the Athabasca oil sands in Canada. The extraction process produces approximately three barrels of process water per barrel of oil, stored in large tailing ponds currently withholding an estimated trillion litres of waste water (Headley *et al.*, 2011, Rowland *et al.*, 2011).

An extractable organic fraction from the oil sand process water is naphthenic acids. Headley *et al.* (2011) investigated the potential leaching of tailing ponds into the local environment such as lakes, using Fourier transform ionisation cyclone resonance mass spectrometry (ESI-FTICR-MS). The instrument has a high resolution and they were able to fingerprint oil contamination from the tailing ponds, distinguishing it from the natural background oil concentrations in river samples. The technique revealed different ratios of polar organic compounds e.g. those containing S, O and NO species, including naphthenic acids. The method was unable to identify specific naphthenic acids or the extent of leaching however ESI-FTICR-MS showed potential as a strong alternative or supporting resolving technique in the analysis of crude oil, especially with further development.

Rowland *et al.* (2011) have been the first to successfully identify individual naphthenic acids in oil sand process waters using GC×GC-TOF-MS. This was achievable due to the highly efficient separation of the GC×GC (1.6 billion theoretical plates) and the removal of bleed ions from the mass spectra; undesired ions from the stationary phase (Rowland *et al.*, 2011).

Their focus was on tricyclic acids which are a main constituent of process water, identifying many compounds by comparing the mass spectra with purchased reference acids. A selection of diamondoid tricyclic acids were structurally identified and uniquely different isomers were characterised such as adamantane-1-carboxylic acid and adamantane-2-carboxylic acid (Rowland *et al.*, 2011). The two isomers had different retention times on the apolar GC column and there was critical analysis of mass spectra which led to distinguishing between tertiary and quaternary fragmentation patterns of the two isomers (Rowland *et al.*, 2011).

1.5 Synthesis of H-Branch Alkanes

Alkanes are classified as saturated hydrocarbons i.e. singly bonded atoms consisting of carbon and hydrogen. Alkanes contain no functional group and are relatively unreactive unless subjected to rigorous conditions e.g. during catagenesis or cracking (Clayden *et al.*, 2001). Alkanes can also be biodegraded by microbial action, for example *Pseudomonas fluorescens* is a microbe known for degrading hydrocarbons in the marine environment (Gough *et al.*, 1992). The biodegradation of aliphatic hydrocarbons, in particular ‘T-branch’ alkanes, has been used to identify

such structures and their degraded counterparts within extracted aliphatic UCMs (Gough *et al.*, 1992, Gough and Rowland, 1990).

Alkanes can have many configurations; straight chain, branched and cyclic, each able to display isomerism (**Error! Reference source not found.**2).The alkanes of interest in this investigation were C_{19} dialkyl alkanes, termed 'H-branch' alkanes. H-branch alkanes consist of three linear carbon chains, interconnected by two tertiary carbons, forming an 'H' shape configuration (**Error! Reference source not found.**).

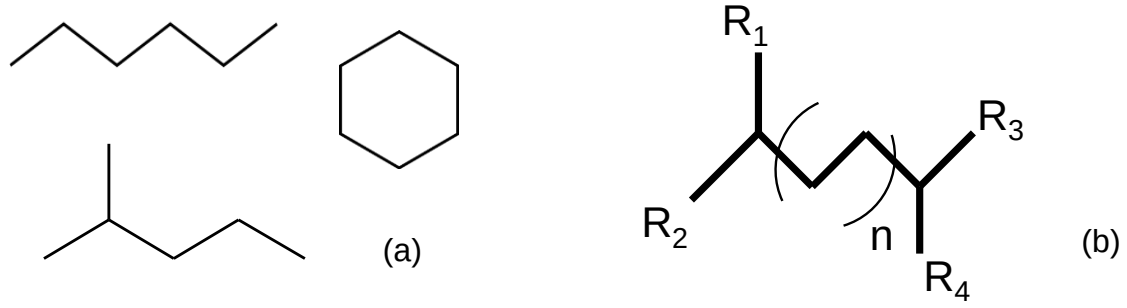

Figure 2: (a) different alkane configurations, (b) general formula for H-branch alkanes

The synthesis of alkyl alkanes has been utilized for the modelling of many branched hydrocarbons discovered naturally, varying from; identifying T-branch aliphatic hydrocarbons in the UCM in lubricating oil feedstocks, authenticating branched aliphatic alkanes in ancient sediments and shales and replicating insect pheromones (Gough and Rowland, 1991, Zarbin *et al.*, 2004, Kenig *et al.*, 2003).

The overall reaction scheme used throughout this investigation was adapted from Gough and Rowland (1991), shown in **Error! Reference source not found.**. First, a tertiary alcohol was synthesised using organometallic reagents i.e. Grignard reagents, coupled with an alkyl halide already consisting of a tertiary carbon (Figure **4**4). The tertiary alcohol was readily dehydrated to form a series of alkene stereoisomers, containing two tertiary carbons. The alkenes underwent hydrogenation over a suitable catalyst e.g. Pd 10%/C to produce the desired alkanes containing two stereogenic centres.

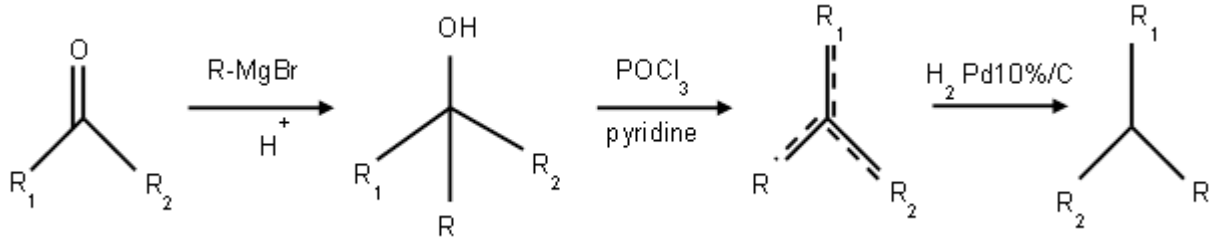

Figure 3: Reaction scheme to synthesise an H-branch alkane

Marukawa *et al.* (2001) took a similar approach, using a Grignard reaction during the synthesis of cuticular hydrocarbons produced by *Diacamma*, a particular ant species. To extend the length of the original carbon chain, they reacted a C_{19} single branched aldehyde with nonyl magnesium bromide, forming the main C_{28} structure of (R)-13-methylheptacosane (Marukawa *et al.*, 2001). The reaction was carried out using THF as the solvent and they obtained a 55% yield (Marukawa *et al.*, 2001).

A similar, alternate method to the general Grignard reaction scheme shown in**Error! Reference source not found.**4, is to react the alkyl halide, carbonyl and magnesium together without the preliminary formation of a Grignard reagent, known as the Barbier reaction which preceded Victor Grignard's commended investigations (Smith and March, 2007).

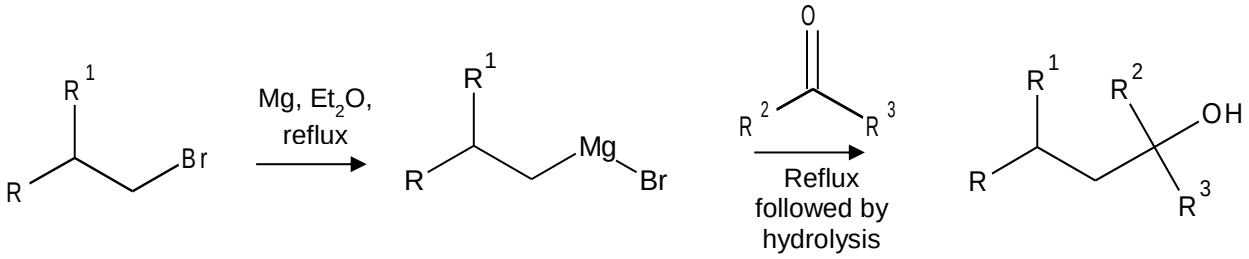

Figure 4: General reaction scheme for a Grignard Reaction producing a tertiary alcohol with two tertiary carbons

Warton *et al.* (1997) synthesised several T-branch alkanes as reference compounds during the identification of single branched alkanes in five crude oils of three different origins; non-marine, marine and deltaic. They synthesised a series of C_{18} T-branched alkanes, increasing the carbon number of the branched alkyl group while reducing the carbon number of the main straight chain (Warton *et al.*, 1997). First, Warton *et al.* (1997) generated tertiary alcohols by reacting suitable Grignard reagents with an ethyl ester; the use of esters in Grignard reactions results in two branches being identical and as a result the tertiary carbon produced was not stereogenic. The tertiary alcohols were dehydrated using phosphoric acid and the variety of alkenes produced were hydrogenated using 10% palladium on carbon as a catalyst; the tertiary carbon was not chiral therefore the final alkanes had no diastereoisomers (Warton *et al.*, 1997).

The synthesis of an H-branch alkane requires the formation of a new carbon-carbon bond, involving carbonyl addition reactions. There are many different reactions that could have been utilized to produce an H-branch alkane, the potential reagents can be determined from the target molecule using retrosynthetic analysis (Clayden *et al.*, 2001) (Figure **5**5). Synthesising a known target molecule allows the structure to be separated into precursor compounds using disconnections. The restriction on disconnections is that they must correspond with achievable reactions e.g. known nucleophilic and electrophilic additions and substitutions (Clayden *et al.*, 2001). If the separated components allow for a choice of reagents but further considerations are required e.g. availability, the idealised compound can be indicated by a synthon. The synthon denotes the necessary fragment of the molecule with the required polarity necessary to react and produce the target molecule (Clayden *et al.*, 2001).

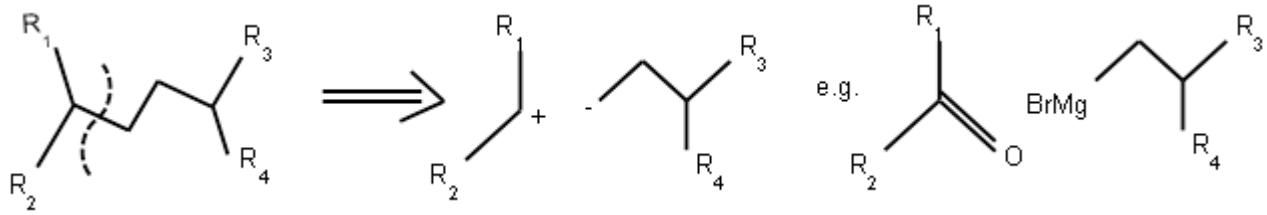

Figure 5: An example of a retrosynthetic approach

Retrosynthesis shows that the addition of Grignard reagents to carbonyl compounds are not the only way to synthesis branched structures. Carbon-carbon bonding reactions also include aldol addition reactions, Claisen condensation reactions and Wittig reactions. Kenig *et al.* (2003) studied the occurrence of branched aliphatic alkanes containing a quaternary carbon, in Late Cretaceous shales and Holocene marine sediments. To authenticate and support their GC-MS results, they synthesised two diethyl pentadecanes; the initial synthesis began with a Wittig reaction. Readily available alkyl phosphonium salts e.g. $CH_3(CH_2)_{10}PPh_3Br$, were converted to their corresponding ylides with butyl lithium, followed by condensing the ylides with the appropriate aldehyde to produce alkenes (Kenig *et al.*, 2003). The aldehydes used already contained the quaternary carbon. The alkenes were hydrogenated using the same catalyst as Warton *et al.* (1997) with H_2/Pd10%/C. The organisms that produce the branched alkanes were undetermined however the geological distribution of the alkanes gives an insight into the type of organisms which create them and the conditions in which they were biosynthesised (Kenig *et al.*, 2003).

Zarbin *et al.* (2004) utilized the Wittig reaction when investigating ant pheromones. They synthesised dimethyl heptadecanes by performing an unsymmetrical double Wittig olefination (Zarbin *et al.*, 2004). A dibromoalkane was converted into a bis-phosphonium salt in DMF, the bis-phosphonium salt subsequently underwent two separate conversions into monoylides; reacting each end of bis-phosphonium salt with the appropriate ketone individually to reduce the formation of symmetric coupling products (Zarbin *et al.*, 2004). This was achieved by reacting 1 equivalent of butyl lithium and a ketone whilst increasing the temperature of the reaction from -90°C to room temperature. Any bis-ylides that formed were believed to react with any remaining bis-phosphonium salt upon increasing the temperature, forming monoylides (Zarbin *et al.*, 2004). The temperature was then reduced back to -90°C and the reaction repeated with a different ketone. The procedure used and the predicted mechanism was justified by performing the procedure without the individual heating and comparing the yields; there was a reduction in symmetric coupling products by nearly 20% (Zarbin *et al.*, 2004).

1.6 Aims and Objectives

The aims of the research project were; to synthesis at least one ‘H-branch’ dialkyl alkane and compare the results and observations with the most recent synthesis techniques and contribute evidence towards the mechanisms and understanding of Grignard reactions, dehydration and hydrogenation reactions. To understand the potential applications of the results; expanding the understanding of the unresolved complex mixture. The desired H-branch, synthesised in this investigation was 5-ethyl-7-butyltridecane (

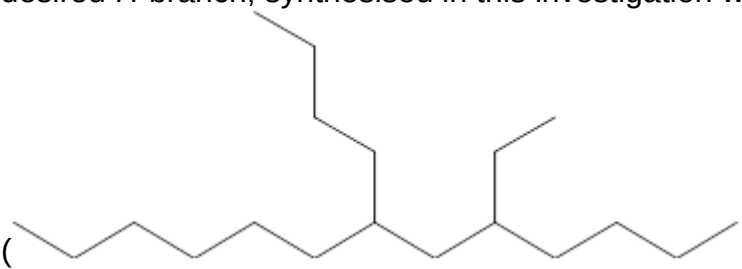

Figure).

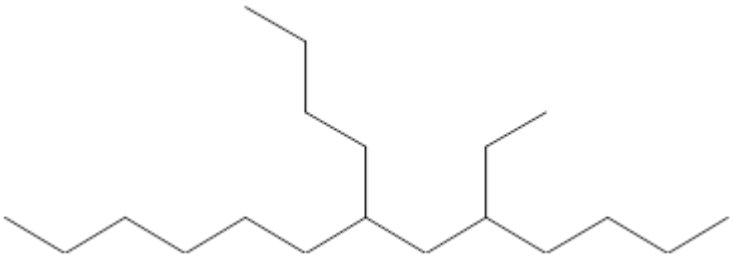

Figure 6: Structure of H-branch alkane, 5-ethyl-7-butyltridecane

The objectives of the investigation were; to perform a series of experiments involving; syntheses, purification techniques, dehydration and hydrogenation. The success of each stage throughout the overall synthesis of the H-branch alkane was verified using analytical instrumentation such as GC-FID and GC-MS accompanied by structural analysis using IR and mass spectrometry. The synthesis implemented good laboratory practical skills and entailed responsible time management.

The review of the literature reveals a clear gap in the knowledge of the synthesis and presence of H-branch alkanes in the UCM. There is no current advanced research in the identification, quantification and toxicology understanding of H-branch alkanes in the unresolved complex mixture. The presence of branched or isoalkanes in crude oil is believed to originate from heavy alkanoic acids i.e. carboxylic acids and esters which undergo decarboxylation during catagenesis, followed by subsequent cracking processes producing alkanes an alkenes, the alkenes then react in acidic clays to form branched alkanes (Kissin, 1987). Isoalkanes constitute for 10-25% of petroleum, predominantly present as mono- or dialkyl alkanes, highlighting the necessity of this project as potentially valuable research (Kissin, 1987).

The research will provide further evidence of the efficiency of Grignard reactions in the production of tertiary alcohols; a practice and actual synthesis of the desired tertiary alcohol was subsequently followed by an adapted synthesis and a comparison of the yields. The results obtained, report the effectiveness of the dehydration and hydrogenation methods implemented and whether they correspond to the literature.

The results have the potential to fill several knowledge gaps about aliphatic toxicity. The research into the toxicity of the UCM has been demonstrated by Donkin et al (2003) focusing on the soluble aromatic fraction of the UCM. Exposing mussels, *Mytilus edulis*, to an extracted monoaromatic UCM from a contaminated site, reduced the feeding rate of juvenile mussels by a considerable 70% (Donkin *et al.*, 2003). Emphasis has also been given to the polar compounds e.g. alkylphenols of the water soluble fraction in biodegraded oil, alongside aromatics e.g. PAHs, the polar compounds have similarly significant toxicological effects verified by exposing male rainbow trout hepatocytes to extracted fractions (Melbye *et al.*, 2009).

Exploration of the aliphatic fraction can be overlooked as non-degraded, long, straight chain alkanes tend to have low solubility and therefore are not considered a toxic threat to marine organisms. However branching of alkanes has been shown to significantly increase the aqueous solubility of heavier alkanes; the branched

analogue of *n*-undecane was shown to increase the solubility from 14 μg L^{-1} to 297 μg L^{-1} (Wraige, 1997).

Aliphatic alkanes can undergo severe microbial degradation and weathering; therefore the synthesised product could be used in determining oxidation or degraded products within the UCM. Thomas *et al.* (1995) showed that weathering and oxidation of aliphatic alkanes produces carboxylic acids, ketones and lactones which are sufficiently soluble to significantly enhance the toxicity of the UCM. Quantitative structure-activity relationships (QSARs); models used to predict chemical properties and the biological response, have confirmed that such oxidation products should be toxic in the environment (Thomas *et al.*, 1995).

2. Materials and Methods

The initial laboratory work involved three separate synthesises; a practice synthesis, a first synthesis of the desired tertiary alcohol and, after analysis of the products, a second synthesis with alterations to investigate and improve the method and results. The synthetic route is outlined in

Figure **7**, the pathway chosen to synthesise the desired product, 5-ethyl-7-butyltridecane, took into account the accessibility, cost and quantities of reagents and the availability of the apparatus and instrumentation.

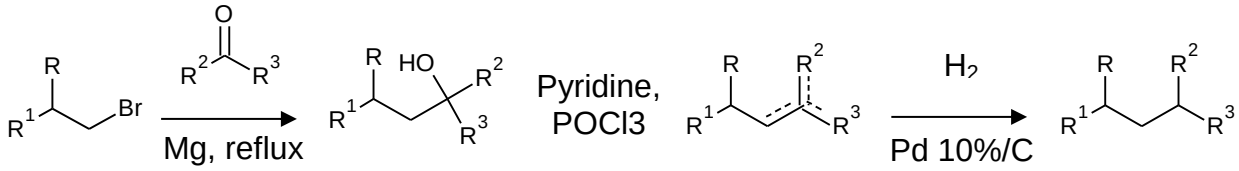

Figure 7: Reaction scheme for the synthesis of 5-ethyl-7-butyltridecane.

2.1 Synthesis of Synthesis of 5-ethylnonan-5-ol

The method for the practice synthesis was adapted from a previous laboratory script supplied in Lewis (2011). The apparatus was oven dried for 24 hours, to remove any moisture before assembling as shown in **Error! Reference source not found.**, in a fume cupboard (Lewis, 2011).

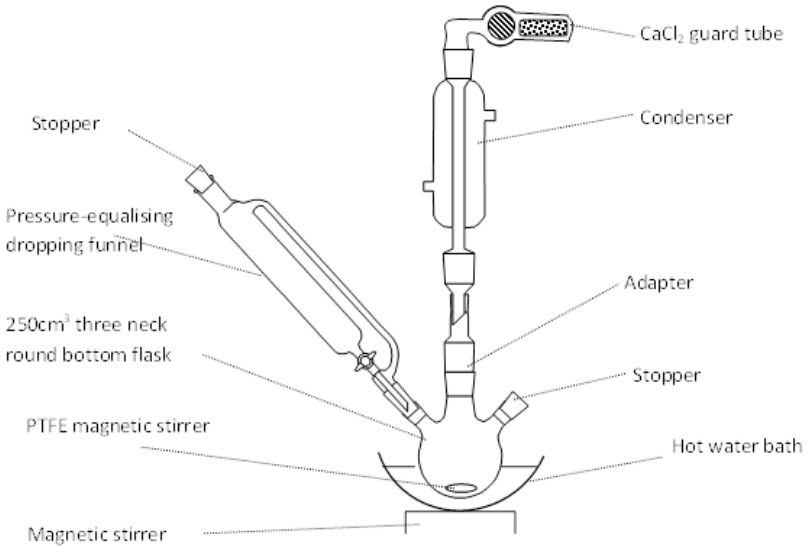

Figure 8: Grignard reaction apparatus set up

Next, magnesium turnings (2.60 g) were weighed and transferred into the 250cm^3 three neck round bottom flask, followed by sodium-dried diethyl ether (50 cm^3). Afterwards, 1-bromobutane (10.7 cm^3, 0.0996 mol) was decanted into the pressure equalising dropping funnel, diluted with sodium-dried diethyl ether (15 cm^3). The funnel was gently shaken to mix the alkyl bromide and diethyl ether, if the funnel was removed from the round bottom flask, the opening was fitted with a glass stopper to reduce moisture entering the system.

To initiate the formation of the Grignard reagent, a few drops of diluted 1-bromobutane were run into the round bottom flask containing the magnesium in diethyl ether whilst heated by a hot water bath. The solution was observed effervescing, becoming turbid and cloudy, forming a grey colour precipitate. The reaction mixture was refluxed for 20 minutes in the practice synthesis but was prolonged for varying times in the subsequent synthesises (Sections 2.2 and 2.3), to explore the effects of reflux time on yield.

Following the complete addition of the alkyl bromide, the hot water bath was replaced with an ice bath. Next, 3-heptanone (14.1 cm^3, 0.101 mol) was poured into the pressure equalising dropping funnel, diluted with another an aliquot of Na sodium-dried diethyl ether (15 cm^3). The dropping funnel was carefully shaken as before, to mix the solutions. The 3-heptanone was added in small aliquots over a period of ten minutes, the colour of the precipitate was observed changing from a dark grey to a light grey. Afterwards the ice bath was replaced with a hot water bath and the reaction mixture was refluxed for a further ten minutes, during which there was vigorous effervescence. The length of the second reflux was also altered in the following synthesises (Sections 2.2 and 2.3).

After the Grignard reagent, butyl magnesium bromide, had finished reacting with the 3-heptanone, the solution was cooled by replacing the hot water bath with an ice bath. The cooled reaction mixture was decanted over the crushed ice (*ca* 57 g) with continuous stirring, whilst avoiding transferring any unreacted magnesium and the

magnetic stirrer. A thick white precipitate formed. An aliquot of anhydrous diethyl ether (10 cm^3) was used to wash the round the bottom flask and excess magnesium, transferring any residing product.

Next, saturated aqueous ammonium chloride (50 cm^3) was transferred into the beaker. On addition, two layers formed; the top ethereal layer containing the white precipitate and a clear aqueous bottom layer containing the by-products of the Grignard reaction. The solution was transferred into a 250cm^3 separating funnel and the two layers were allowed to separate. An emulsion formed at the bottom of the ethereal layer. The aqueous layer was collected in the beaker and the top layer including the emulsion was collected in a 250cm^3 conical flask. The aqueous layer was washed and re-extracted with two more aliquots (20 cm^3 each) of anhydrous diethyl ether. The top ethereal layers were collected and combined in the conical flask.

Following the extraction, anhydrous potassium carbonate was added to the combined ether solution, containing the product. The anhydrous potassium carbonate dried the solution and removed the emulsion seen during the separation. The conical flask was stoppered and stored in a dark cupboard, left to dry overnight.

After drying, the solution was filtered under gravity through fluted filter paper into a pre-weighed round bottom flask. When filtration was complete, rotary evaporation was performed on the filtrate to remove the ether solvent. The solution became a pale yellow colour with an increased viscosity and strong fruity aroma indicating the presence of unreacted ketone in the crude product. Subsequently, the mass of product (13.03 g) and crude yield was determined, the crude product was analysed by IR, GC-FID and GC-MS.

2.2 First synthesis of 5-ethyl-7-butyltridecan-7-ol

The procedure for the first synthesis of 5-ethyl-7-butyltridecan-7-ol was similar to previous practice synthesis adapted from a previous practical script supplied in Lewis (2011). Due to the limited availability of 5-undecanone the reaction was carried out at a lower molar ratio.

The apparatus was set up as shown in **Error! Reference source not found.**. The mass of magnesium (2.62 g) despite similar to the practice experiment, was in greater excess compared to the volume of alkyl bromide. A small aliquot of 2-ethylhexylbrominde (2.7cm^3, 15.2 mmol) was diluted in sodium-dried diethyl ether (15 cm^3) and decanted into a 100 cm^3 pressure equalising funnel.

The initiation of the Grignard reagent took longer than before, with no observable changes after 10 minutes with the addition of several aliquots of 2-ethylhexylbromide. A glass rod was used to scrape the magnesium turnings in an attempt to remove any oxide layer, to expose and increase the fresh magnesium surface area. The additional scrapping along with the replacement of the hot water bath succeeded in starting the reaction, indicated by turbidity, effervescence and a white grey precipitate. The solution was refluxed for a further 20 minutes.

After the complete addition of the alkyl bromide, 5-undecanone (3.0 cm^3, 14.6 mmol) was added over 10 minutes and allowed to reflux for a further 20 minutes. The volumes of sodium- dried diethyl ether were kept the same as the practice

experiment, however relative to the quantity starting reagent; the dilutions were much greater in an attempt to improve the yield.

The work up using saturated aqueous ammonium chloride (50 cm^3) and separation step was the same as the practice investigation (Section 2.1), except no emulsion was observed between the ethereal and aqueous layer. The crude product was dried with anhydrous potassium carbonate, rotary evaporated, weighed (3.23 g) and analysed by IR, GC-FID and GC-MS.

2.3 Second Synthesis of 5-ethyl-7-butyltridecan-7-ol

The apparatus was rinsed with diethyl ether and oven dried for 24 hours before being set up as shown in **Error! Reference source not found.**, containing the main assembly of the apparatus within the oven before transferring to the fume cupboard to reduce the moisture content within the system. The stoppers were only removed when decanting the solutions and replaced afterwards.

The procedure followed was similar to the first synthesis but the stages identified as responsible for the resulting product were adapted to improve the yield, including; the mass of magnesium, the addition and reflux time of alkyl bromide, the initiation of Grignard formation and the addition and reflux period of the ketone. The sodium-dried diethyl ether dilutions were kept the same however a lower quantity of 5-undecanone was available.

To maintain the desiccate conditions, the magnesium (2.73 g) was dried in the oven for 10 minutes prior the transferring it into the round bottom flask. After decanting 2-ethylhexyl bromide (2.7 cm^3, 15.2 mmol) diluted with diethyl ether (15 cm^3) into the pressure equalising funnel, a small aliquot was run into the round bottom flask to initiate the reaction. There were no observable changes after 30 minutes, further small aliquots of alkyl bromide were added during this period however the starting concentration of alkyl bromide was kept lower than in the previous experiment as an attempt to maintain a favourable equilibrium when the formation of Grignard reagent did begin. An iodine crystal was added to activate the magnesium, turning the solution orange and the hot water bath was replaced.

The addition of an iodine crystal was successful, the solution turned clear than turbid, effervescing and a grey white precipitate was observed. The complete addition of the 2-ethylhexyl bromide was carried out over 30 minutes and the solution was refluxed for a further 30 minutes, different from the previous synthesis. The precipitate was a darker grey and there was vigorous effervescence.

After cooling the reaction in an ice bath, 5-undecanone (2.2 cm^3, 10.7 mmol) in Na dried diethyl ether (15.0 cm^3) was added over a 15 minute period followed by 20 minutes of refluxing with a hot water bath. The dark grey precipitate became a light grey/white precipitate.

After completing the reaction, the work up with saturated aqueous ammonium chloride (50 cm^3) and separation technique was kept the same as Sections 2.1 and 2.2. There was no emulsion observed in the ethereal layer and the crude product was dried with anhydrous potassium carbonate. After filtration and rotary evaporation and determining the crude mass of product (2.08 g) and yield, the product analysed by IR, GC-FID and GC-MS.

2.3 Purification by Column Chromatography

Column chromatography was performed on the second synthesis product to purify and isolate the desired 5-ethyl-7-butyltridecan-7-ol from the possible by-products and unreacted starting materials e.g. Wurtz-coupling product, ketone and alcohol.

The apparatus was set up as shown in Figure.

Packing the column involved preparing a slurry of silica with hexane as an effective way of transferring the silica into the column. Gentle shaking encouraged the removal of air bubbles as the silica compacted and settled on top of the sintered glass frit. The excess hexane was run through until the level was just above the silica; the silica was kept saturated with solvent throughout the experiment to avoid drying and cracking which can ruin the separation.

The crude product was evenly transferred on to the surface of the silica with a Pasteur pipette avoiding the column sides, the round bottom flask containing the product was rinsed with a few aliquots (few cm^3) of hexane and also transferred onto the silica column. Afterwards, filter paper was placed on top of the silica to reduce disturbing the column when decanting additional solvent.

The separation involved running an eluotropic series; beginning with hexane and increasing the polarity after a few fractions of each, using 5, 10, 15, 20, 30, 50 and 100% diethyl ether followed by 100% methanol. Each fraction was collected in a round bottom flask, a small aliquot of sample was dotted on a TLC plate and tested for fluorescence and any eluate containing product was identified by recording the mass of the fraction after rotary evaporation.

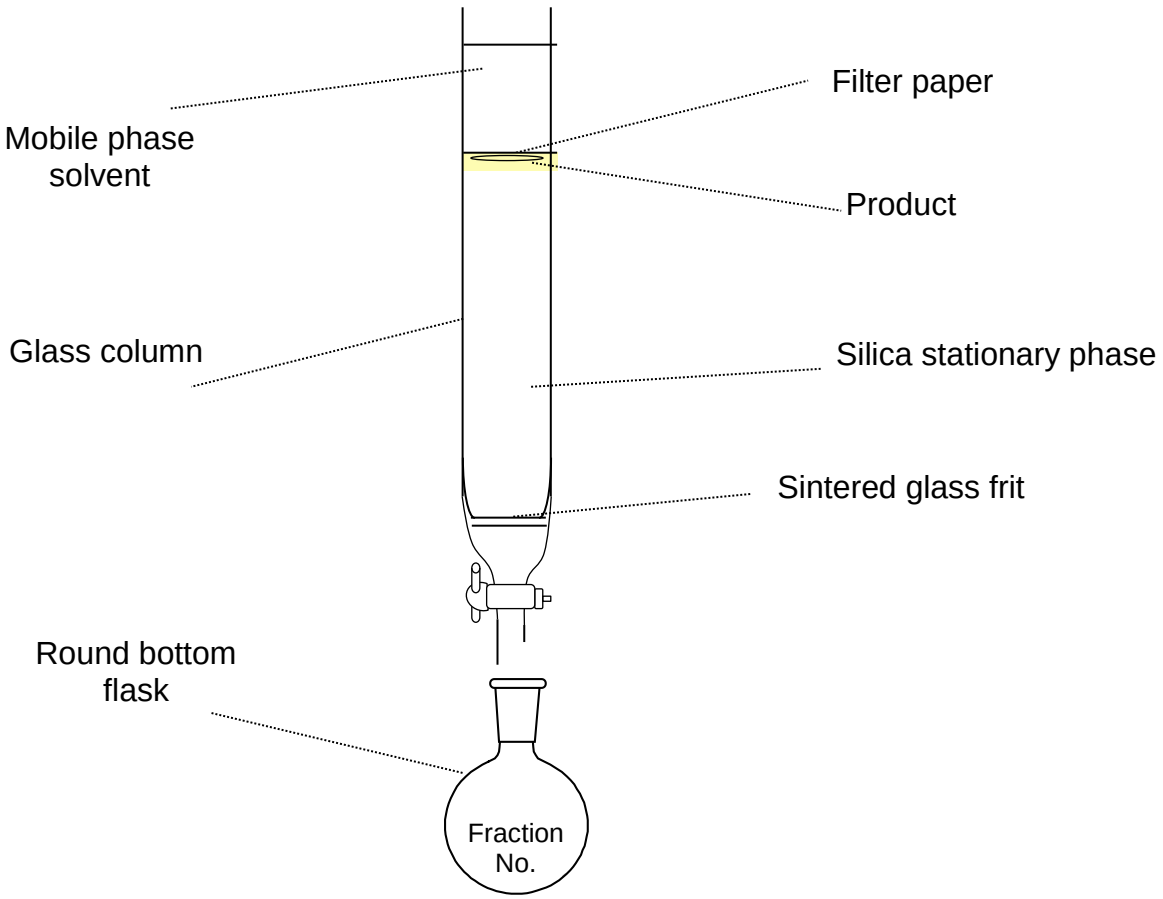

[65]

Figure 9: Assembly of column chromatography apparatus

After separation, fractions with a significant mass or visible product were retained. To gain an accurate mass of each fraction, the fractions were transferred into separate pre-weighed 7cm^3 glass vials, the round bottom flasks were rinsed with several aliquots of hexane and transferred into the vials. The solvent was removed by nitrogen blow down (40°C) and the vials were reweighed. The accurate masses were used to plot a gravimetric analysis graph.

The fractions believed to contain the first elution of the alcohol and the final elution were analysed by IR to give an indication of any change in chemical structure across the fractions.

Samples with the highest masses and samples indicating the beginning and end elution of different fractions, covering a representative portion of the fractions, were analysed by GC-FID and GC-MS (see Section 2.6).

2.4 Synthesis of 5-ethyl-7-butyltridecenes

After purification of 5-ethyl-7-butyltridecan-7-ol and analysis of the fractions using GC-MS, fractions 20 and 21 were identified as containing most of the product with a small quantity of ketone. Fractions 20 and 21 were combined into one glass vial using several aliquots of hexane (~2 cm^3 ×4) to ensure a quantitative transfer of product, the solvent was removed by nitrogen blow down (45 min at 40°C).

The glassware used in the assembly of the dehydration apparatus were rinsed with DCM and allowed to dry prior to use. The combined fraction was weighed (0.1471 g) and transferred into a 25 cm^3 round bottom flask. Next, a small volume pyridine (1.2 cm^3) was transferred into the round bottom flask; a portion of the pyridine (×4 small aliquots) was reserved for repeated rinsing of the glass vial to transfer any remaining product into the round bottom flask.

An ice bath was prepared and placed on top of a magnetic stirrer, the stirrer bar was placed in the round bottom flask, which was then fitted with an air condenser and secured in the ice bath. The product/pyridine solution did not solidify upon cooling, and remained dissolved in the pyridine. After assembling the apparatus, a small aliquot of $POCl_3$ (0.8 cm^3) was measured and decanted into a 25 cm^3 glass beaker. Using a long stemmed glass Pasteur pipette, the $POCl_3$ was added cautiously, drop wise through the top of the air condenser into the round bottom flask. The initial drops resulted in a vigorous exothermic reaction with the release of white plumes of smoke which reduced as the reaction proceeded followed by the formation of an off-white, light beige precipitate being observed in the solution. When all of the $POCl_3$ was added, a few drops of pyridine were used to wash down the residue that had collected on the sides of the air condenser; this resulted in a prompt, vigorous evolution of more white smoke.

The top of the air condenser was fitted with a $CaCl_2$ guard tube to reduce the amount of moisture entering the system while the reaction was left to proceed in the ice bath overnight. The reaction mixture had become mainly precipitate by the following

morning and the ice bath had melted. Next, hexane (10 cm^3) was decanted through the top of the air condenser to rinse the sides of the condenser and dissolve the precipitated product, achieved by swirling the round bottom flask. A glass rod was used to scrape the precipitate to allow the magnetic stirrer to rotate and mix the solution. Then the dissolved reaction mixture was poured over ice (*ca* 20 g) in a 150 cm^3 glass beaker. After gently swirling, the solution was transferred back into the round bottom flask, swirled and decanted into a 50 cm^3 separating funnel. During the addition of the $POCl_3$, the glass stem from a Pasteur pipette broke and fell into the round bottom flask; the fragment was rinsed with hexane and removed.

Subsequent rinsing of the round bottom flask (3 cm^3 ×2), glass beaker, glass rod, magnetic stirrer (collectively with 3 cm^3×2) and air condenser (3 cm^3) was carried out with hexane and the washings poured into the separating funnel.

The reaction/hexane mixture was allowed to separate and two layers were observed, before running the bottom aqueous layer into a 150 cm^3 glass beaker and collecting the top organic, hexane layer in a 50 cm^3 conical flask. The aqueous layer was re-extracted with several aliquots of hexane (4 cm^3×6), which were all combined in the conical flask.

The combined hexane solution was decanted back from the conical flask into the separating funnel and was washed with 2M HCl (3 cm^3×3) and deionised water (3cm^3×3). Each washing involved shaking the separating funnel, allowing the layers to separate and removing the bottom aqueous layer before adding the following volume of HCl or deionised water. After washing, the hexane solution was collected in the 50 cm^3 conical flask with the addition of Na_2SO_4 drying agent. The solution was left to dry overnight.

After drying, the hexane solution was filtered under gravity through fluted filter paper into a pre-weighed 100 cm^3 round bottom flask. A few crystals of drying agent had passed through with the filtrate therefore a small volume of hexane was removed by rotary evaporation and the hexane solution was filtered again into a different pre-weighed round bottom flask. The remaining solvent was removed by rotary evaporation and the mass of product was recorded (0.0911 g). The product was analysed by GC and GC-MS.

2.5 Synthesis of 5-ethyl-7-butyltridecane

After the dehydration was proved successful in the syntheses of 5-ethyl-7-butyltricene(s) confirmed by GC and GC-MS, the mixture of alkenes was ready for hydrogenation. First a solution of 50% ethyl acetate in hexane was prepared, transferring a volume (50 cm^3) into a 100 cm^3 round bottom flask followed by a magnetic stirrer bar. The round bottom flask and stirrer bar had been washed with small aliquots of the 50% ethyl acetate:hexane solution.

A small mass of 10% palladium on carbon catalyst (~0.5 g) was weighed and transferred into the round bottom flask; on addition the solution turned an opaque black colour. The apparatus was assembled as shown in Figure, which allowed hydrogen to bubble through the solution for effective hydrogenation. The two glass traps containing 50% ethyl acetate in hexane ensured the hydrogen gas was saturated with the solvent prior to bubbling through the solution, if the precaution was not taken the hydrogen gas would evaporate the solution. The product/catalyst solution was left to hydrogenate for around six hours.

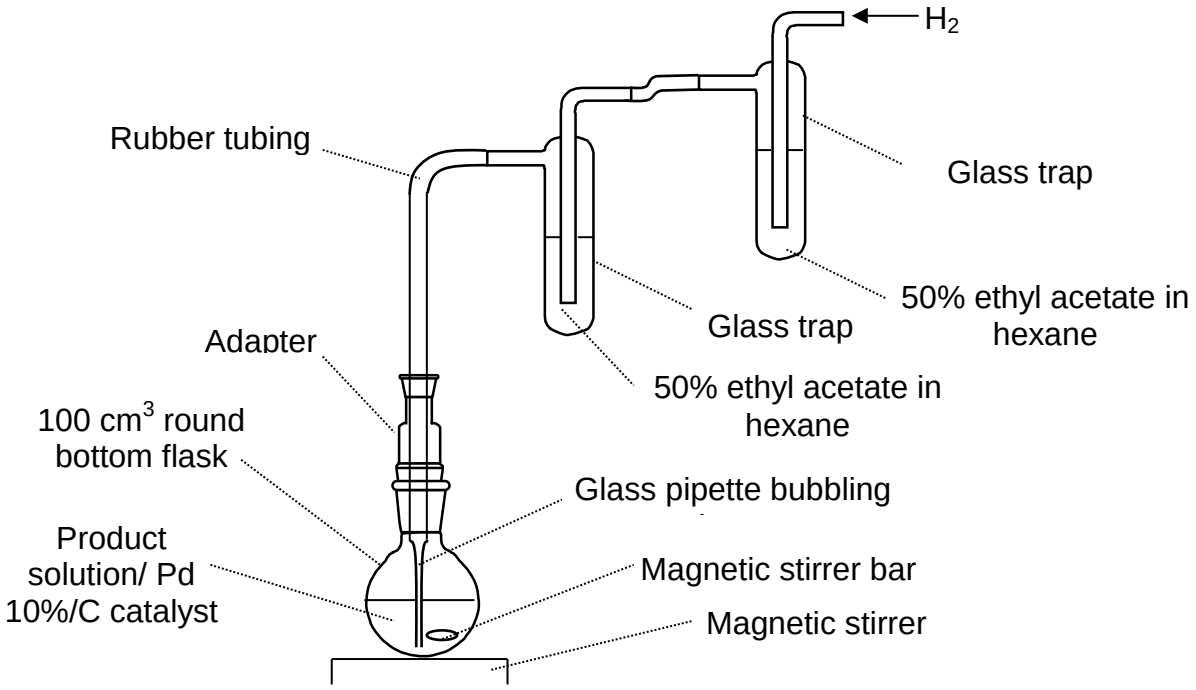

Figure 10: Assembly of hydrogenation apparatus

After the solution had been hydrogenated, the round bottom flask was removed from the hydrogenation system. The solution containing the product and catalyst was filtered under gravity through fluted filter paper (Number 5 fine filter paper) into a previously hexane rinsed, pre-weighed 150 cm^3 round bottom flask. The flask originally containing the solution as rinsed with hexane (few cm^3 aliquot×4) to transfer any residing product.

The filtrate was rotary evaporated to remove the ethyl acetate/hexane solvent, the mass of product (0.0526 g) and yield was determined and followed by subsequent analysis with GC-FID and GC-MS.

2.6 Instrumentation and Conditions

2.6.1 Analysis by FT-IR

The FT-IR analysis was performed using a Bruker Alpha FT-IR spectrometer with a Platinum ATR module. The spectra were attained at 4 cm^{-1} resolution using a DTGC detector, running 16 scans per spectrum.

2.6.2 Analysis by GC-FID

The GC-FID samples had a desired concentration ~250 mg L^{-1}. However, to conserve solvent and time, ~1.25 mg of desired product was weighed into 7 cm^3 glass vials and diluted to 5 cm^3 with hexane. To calibrate the vials, a 5 cm^3 aliquot of hexane was measured and transferred into a vial and used as a blank; the meniscus was marked with a line and the line was reproduced on the subsequent vials. The mass of product in each sample was recorded to calculate the concentration. An aliquot, ~1 cm^3 of each sample was transferred into GC glass vials and analysed.

The instrumentation used was an Agilent Gas Chromatograph 7890A equipped with a 7683 Series Autosampler and 7683B Series Autoinjector. The column was a HP5, 5% phenyl – 95% dimethylsiloxane, low polarity column, 30 m× 0.320 mm internal diameter with a 0.25 µm film thickness. The carrier gas was nitrogen with a flow rate of 1.0 mL min^{-1} and the injector temperature was 250°C. The GC had a flame ionisation detector attached with a temperature of 300°C, hydrogen flow rate of 40 mL min^{-1}, air flow rate of 400 mL min^{-1} and nitrogen (make-up) flow rate of 15 mL min^{-1}. A 'General method' temperature programme was used which ran 40-300°C at 10°C/min and held at 300°C for 10 min. The chromatograms were recorded using Chemstation™ (Revision B.03.01, May 2007) software, able to export to Excel for formatting purposes.

2.6.3 Analysis by GC-MS

The GC-MS samples had a desired concentration of ~25 mg L^{-1}, achieved by diluting 1.0 cm^3 of each GC sample to 10.0 cm^3 in a 10 cm^3 glass volumetric flask with hexane. An aliquot, ~1 cm^3 of each diluted sample was transferred into GC-MS glass vials and analysed. An alternative method for preparing GC-MS samples was to dilute 0.1cm^3 of the GC sample into 1.0 cm^3 of hexane, using a 100 µL glass syringe, in the GC-MS glass vials.

The instrumentation used was an Agilent GC-MSD; 7890A gas chromatograph fitted with a 7683B Series autosampler and a 5975A quadrupole mass selective detector. The column was a HP-5MS fused silica capillary column, 30 m ×0.25 mm internal diameter with a 0.25 µm film thickness. The helium carrier gas was kept at a constant 1.0 mL min^{-1} and a 1.0 µL sample was injected into a 300°C splitless injector. The oven was programmed to rise from 40-300°C at 10°C min^{-1} and hold at 300°C for 10 minutes. The ion source in the quadrupole detector was at 280°C and produced an ionisation energy of 70eV. The chromatograms were recorded using ChemStation™ and the instrument was operated in full scan mode, with 50-550 Daltons monitored, 3 times a second.

3. Results and Discussion

3.1 Synthesis of 5-ethylnonan-5-ol

The synthesis of 5-ethylnonan-5-ol via a Grignard reaction was a practice, preparation step before the actual synthesis of 5-ethyl-7-butyltridecan-7-ol (**Figure**). The structure of 5-ethylnonan-5-ol represents a monoalkyl branched tertiary alcohol with a similar structure to the precursor compounds synthesised by Gough et al. (1990) in the synthesis of 'T- branch' alkanes. Despite 5-ethylnonan-5-ol not being a precursor for H-branch compounds, the smaller T-branch molecule is a tertiary alcohol and would produce an outcome representative of 5-ethyl-7-butyltridecan-7-ol during the water/NH_4Cl work-up. The starting reagents, 3-heptanone and 1-bromobutane, were also readily available, low costing and the reaction was expected to give a high yield allowing for the practice of further analysis such as GC-FID.

Performing a Grignard reaction requires attention to detail, care and previous planning to ensure desiccate conditions throughout initial stages e.g. rinsing and thoroughly drying all glassware 24 hours before the experiment. Carrying out a practice experiment gave an indication of the time required and highlighted any ways to utilize the time more efficiently to improve organisation and time management.

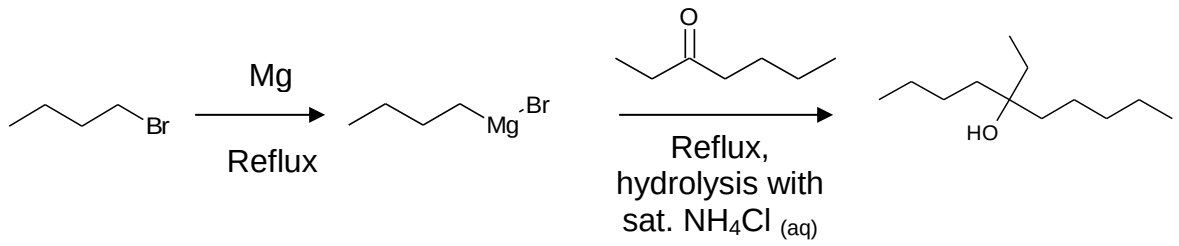

Figure 11: Reaction scheme for the practice synthesis of 5-ethylnonan-5-ol

The limiting reagent of the reaction was the alkyl halide, 1-bromobutane (0.0996 mol), initiating the formation of the Grignard reagent i.e. butyl magnesium bromide, in the presence of excess magnesium turnings (2.60 g). The reaction produced a reasonably high mass of crude product (13.03 g) corresponding to a crude yield of 76%. The GC results showed a purity of 76% and 5-ethylnonan-5-ol had a retention time around 10 min.

The reduced purity was initially thought to be excess 3-heptanone (18%) and a small conversion to its corresponding secondary alcohol (3-heptanol, 5%), displayed as two peaks at 6.206 and 6.312 min. The conversion of the ketone to its alcohol occurs as a side reaction (Smith and March, 2007).

The formation of the Grignard reagent was almost immediate following the first addition of the alkyl bromide to magnesium in diethyl ether (**Figure**). The initial formation was observed as slight effervescence and the appearance of a grey precipitate; the reaction became progressively more vigorous with further additions of alkyl bromide. This observation, of increasing turbidity, is very distinctive of a Grignard formation, originally reported by Victor Grignard in 1900 who observed a cloudy solution while investigating organomagnesium compounds (Kürti and Czakó, 2005).

The Grignard reagent reacts with the ketone by nucleophilic addition. Considering that the carbon atom in the C-Br bond of the alkyl halide originally begins slightly positively charged due to the electronegativity of the bromine atom, there must be a change in polarity. The alkyl halide undergoes oxidative insertion or addition, where the Mg(0) metal inserts itself between the carbon and halogen to form a C-Mg-Br bond (Clayden *et al.*, 2001). The magnesium is thought to react with the halogen first, forming Mg(I)Br and an alkyl radical, which then proceeds to form C-Mg(II)-Br (Komiya, 1997). The C-Mg bond is very polar due to the electropositive magnesium and as a result the carbon atom undergoes a polarity reversal known as ‘umpolung’, becoming partially negatively charged and therefore nucleophilic (Mayo *et al.*, 2000, Kürti and Czakó, 2005). Understanding the nucleophilic character is critical when using organometallics in synthesis; the correct metal should be selected specifically for the types of starting materials and can alter the overall outcome of the reaction. An organomagnesium compound i.e. a Grignard reagent, was suitable for the synthesis of the tertiary alcohol in this investigation (Section 3.2) as the alkyl halide and ketone were relatively simple and low steric hindrance but if other complex starting materials were used, more basic organolithiums or less reactive organoceriums would have been considered (Clayden *et al.*, 2001).

After the formation of the Grignard reagent, refluxing was stopped and the 5-undecanone was added. There were no obvious observations when adding the

ketone to the Grignard reagent or during the reflux that followed, except the dark grey precipitate became a light grey colour. The nucleophilic addition involves the nucleophilic carbon of the Grignard reagent attacking the partially positively charged carbon of the ketone. The C=O moiety has a highly polarised bond caused by the electronegative oxygen atom (Kürti and Czakó, 2005). The nucleophilic addition also proceeds due to the Lewis-acidic character of the magnesium atom; the magnesium is able to accept a lone pair of electrons from the oxygen atom of the ketone, partially catalysing the reaction forward (Clayden *et al.*, 2001).

After the addition of 3-heptanone, the reaction mixture underwent a work-up where water hydrolysed the magnesium alkoxide to produce the desired tertiary alcohol and a magnesium salts (Smith and March, 2007). An acid is usually utilized during the work-up as a catalyst, however an acid could protonate the basic Grignard reagent producing an undesired alkane and it could also dehydrate the tertiary alcohol producing alkenes. To reduce dehydration, saturated ammonium chloride solution was used instead to act as a mild acid, in which the magnesium salts are soluble in, thus they could be separated using simple solvent extraction (Garner, 1997).

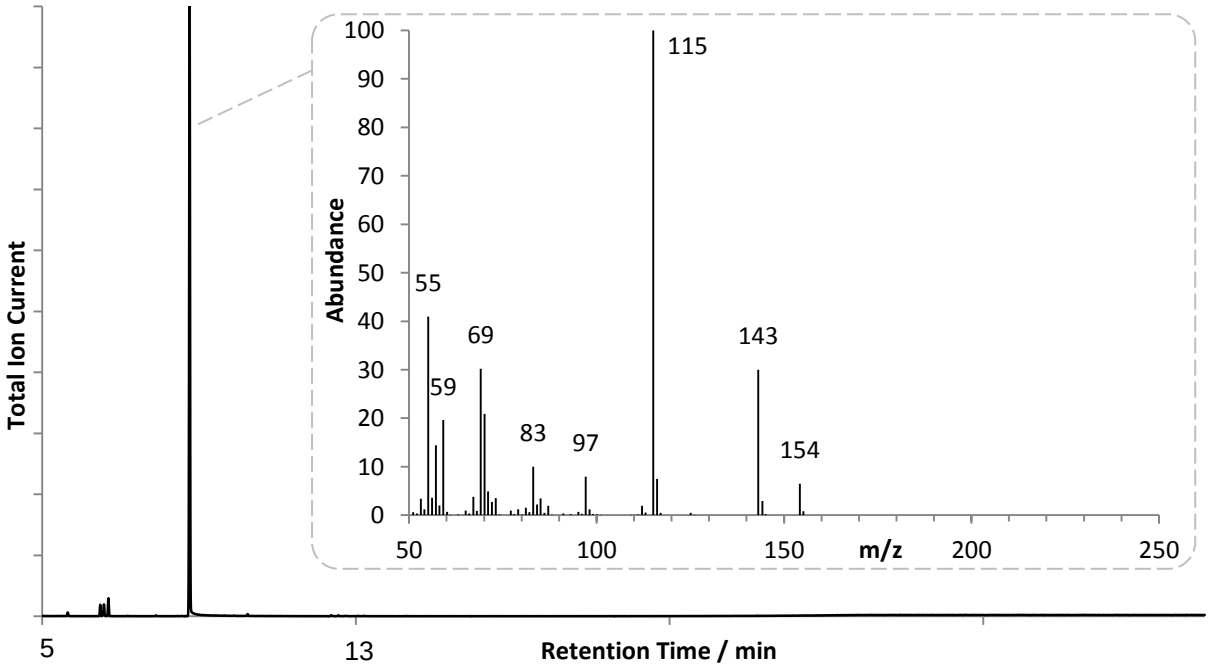

Figure 12: GC-MS chromatogram of practice product and mass spectrum identifying 5-ethylnonan-5-ol

The chromatogram and mass spectrum of the crude product confirmed that the elution around 9 min was 5-ethylnonan-5-ol and that the desired tertiary alcohol had

been successfully synthesised (Figure 12). The retention time was slightly lower during the GC-MS compared to the GC due to variation in the conditions and columns. The very low abundance of the molecular ion peak, $M^{+\cdot}$ = 172 is characteristic of tertiary alcohols as they dehydrate during GC-MS (discussed in Section 3.2), to give an alkene, $M^{+\cdot}$-18 = m/z 154. Further evidence of dehydration was the peaks at m/z 97 and 69 which result from secondary fragmentation of the alkene; m/z 97 corresponding to the loss of a butyl group ($M^{+\cdot} - H_2O - 57$).

The base peak at m/z 115 ($M^{+\cdot} - C_4H_9\cdot$), was a result of α-cleavage i.e. fragmentation of the butyl groups either side of the quaternary carbon (**Figure 12**). The high abundance of the base peak (m/z 115) relative to lower intensity of the m/z 143 ion ($M^{+\cdot} - C_2H_5\cdot$) suggests the presence of two butyl groups and only one ethyl group within the compound (**Figure**). The α-cleavage of the ethyl group, $M^{+\cdot}$- 29 = 143; is observed to a lesser extent because it is a smaller substituent and the radical produced is less stable (Smith, 2004) (**Figure**).

If all the substituents of a tertiary alcohol are alkyl groups, it is not the stability of the ion produced that determines the fragmentation because the stability of the positive charge on the tertiary carbon is similar. The preferential loss, is the alkyl group with the most stable radical supported by Stevenson's rule (Smith, 2004). The butyl radical is more stable than the ethyl radical because of inductive stabilisation effects, thus more likely to fragment (Smith, 2004).

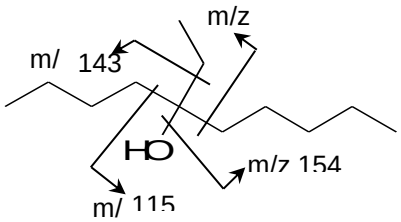

Figure 13: Fragmentation of 5-ethylnonan-5-ol; dehydration and α-cleavage of the tertiary alcohol

The three peaks with low abundance, seen in the chromatogram at a shorter retention time than the tertiary alcohol are evidence of the product undergoing dehydration during the GC column. The three peaks represent a series of 5-ethylnonene isomers, with molecular ions $M^{+\cdot}$ = 154 which corresponds to the dehydrated peak in **Figure 12**.

The impurities shown in the GC-FID chromatogram, eluting at 6.206 and 6.312 min were not structurally identified by GC-MS as the compounds eluted too close to the solvent peak. The GC-MS instrument was programmed to begin recording the chromatogram 5 minutes after the injection as the solvent peak was not of interest and its high abundance distorts the relative intensities of the compounds of interest.

Despite this, comparison of the IR spectra of the starting materials and product suggest that the impurity was excess 3-heptanone (**Figure**). The broad, weak band at 3417.96 cm^{-1} indicative of an –OH stretch and the absorption at 1145.10 cm^{-1} corresponding to a C-O stretch in tertiary alcohols, was preliminary confirmation that the alcohol had been synthesised, verified by the GC-MS mass spectra (Figure 12

and **Figure**). However there were several bands in the IR spectrum of the product that matched almost identical bands in the IR spectrum of 3-heptanone, such as the C=O stretch at 1712.97 cm^{-1} representative of ketones and the absorptions at 970.57 cm^{-1} and 916.44 cm^{-1} in the fingerprint region (Günzler and Gremlich, 2002).

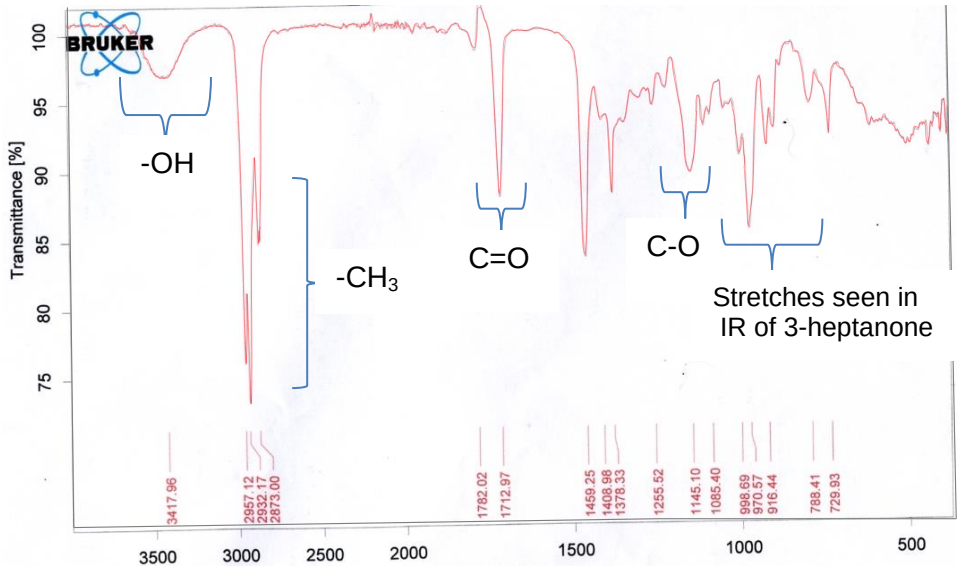

Figure 14: IR spectrum of 5-ethylnonan-5-ol

3.2 Syntheses of 5-ethyl-7-butyltridecan-7-ol

After successfully synthesising 5-ethylnonan-5-ol, achieving a high yield (76%) with reasonable purity (76%), the first synthesis of 5-ethyl-7-butyltridecan-7-ol was carried out. The starting materials were 5-undecanone and 2-ethylhexyl bromide, the quantity of 5-undecanone was limited therefore additional care was taken when working with lower concentrations to reduce contamination. After analysis of the product by IR, GC-FID and GC-MS, the synthesis was repeated using an adapted procedure in an attempt to improve the yield and purity. The reaction scheme for the synthesis of 5-ethyl-7-butyltridecan-7-ol is given in Figure.

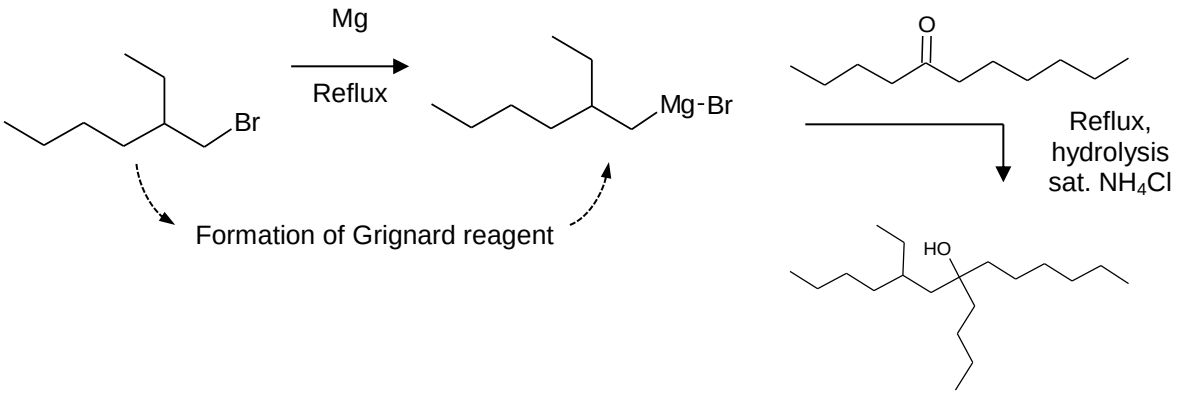

Figure 15: Reaction scheme for the synthesis of 5-ethyl-7-butyltridcan-7-ol

The first synthesis of 5-ethyl-7-butyltridecan-7-ol produced a high, crude mass of product (3.23 g) with a yield (77%) similar to the practice synthesis. However the GC showed the product had a low purity of 6.9% as the product predominantly consisted of excess, unreacted 5-undecanone (56%) and significant a conversion of the Grignard reagent to the Wurtz-type coupling by-product (20%). There was also

contamination during preparation of the GC sample with a plasticiser peak eluting at a very long retention time (3%).

The second synthesis was altered after researching methods to improve the yield of Grignard reactions, however the available starting volume of 5-undecanone was reduced again so additional care was taken to avoid contamination. The second synthesis of 5-ethyl-7-butyltridecan-7-ol produced a lower mass of crude product (2.08 g) and crude yield (68%) however the purity of 12.3% was considerably increased. The overall result meant the adapted procedure employed for the second synthesis was successful in increasing the yield of 5-ethyl-7-butyltridecan-7-ol.

During GC-MS, tertiary alcohols readily undergo dehydration either within the GC column or the mass spectrometer. This was observed in Figure 16 and **Figure 17** by the appearance of four peaks with a similar but shorter retention time than the alcohol, representing the isomeric alkenes. The alcohol peak displayed tailing, characteristic of polar compounds and the structure was confirmed by the mass spectra in **Error! Reference source not found.**. The GC of the second synthesis product showed larger peak intensities of the dehydrated alkenes; this does not necessarily imply that the second product experienced greater dehydration. The alcohol peak of the second synthesis product underwent extensive tailing misrepresenting the intensity of the alcohol peak relative to the quantity of alkene (Figure 17).

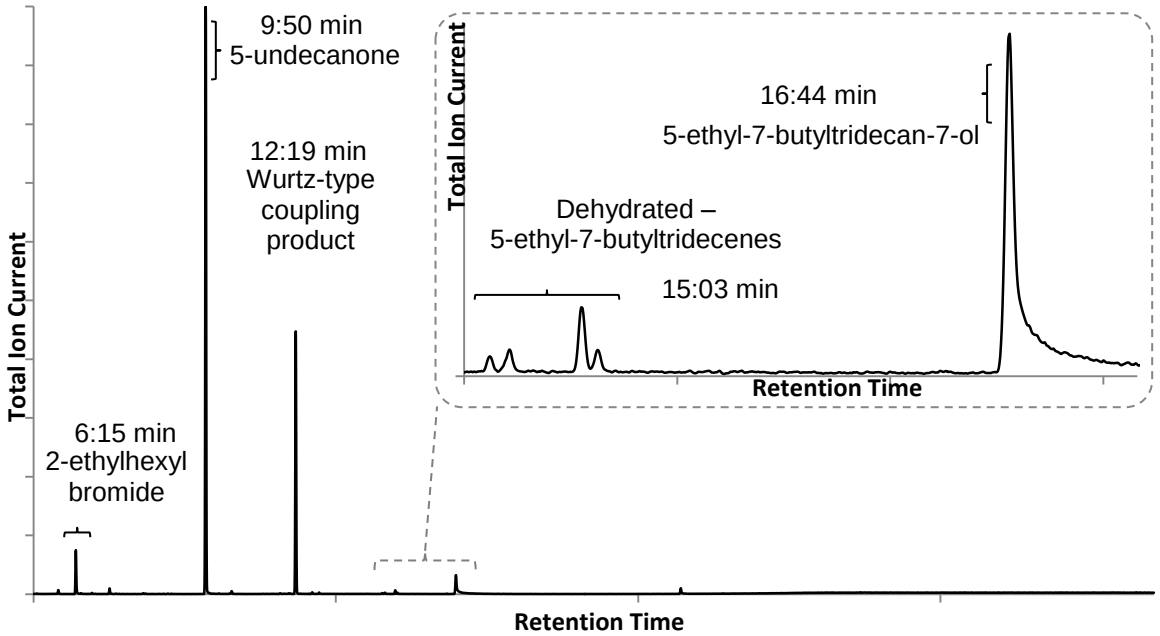

Figure 16: GC-MS chromatogram of 5-ethyl-7-butyltridecan-7-ol from the first synthesis

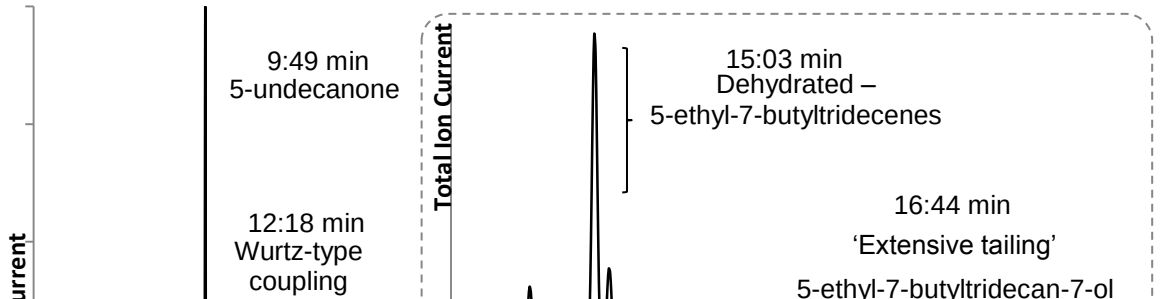

Figure 17: GC-MS chromatogram of 5-ethyl-7-butyltridecan-7-ol from second synthesis

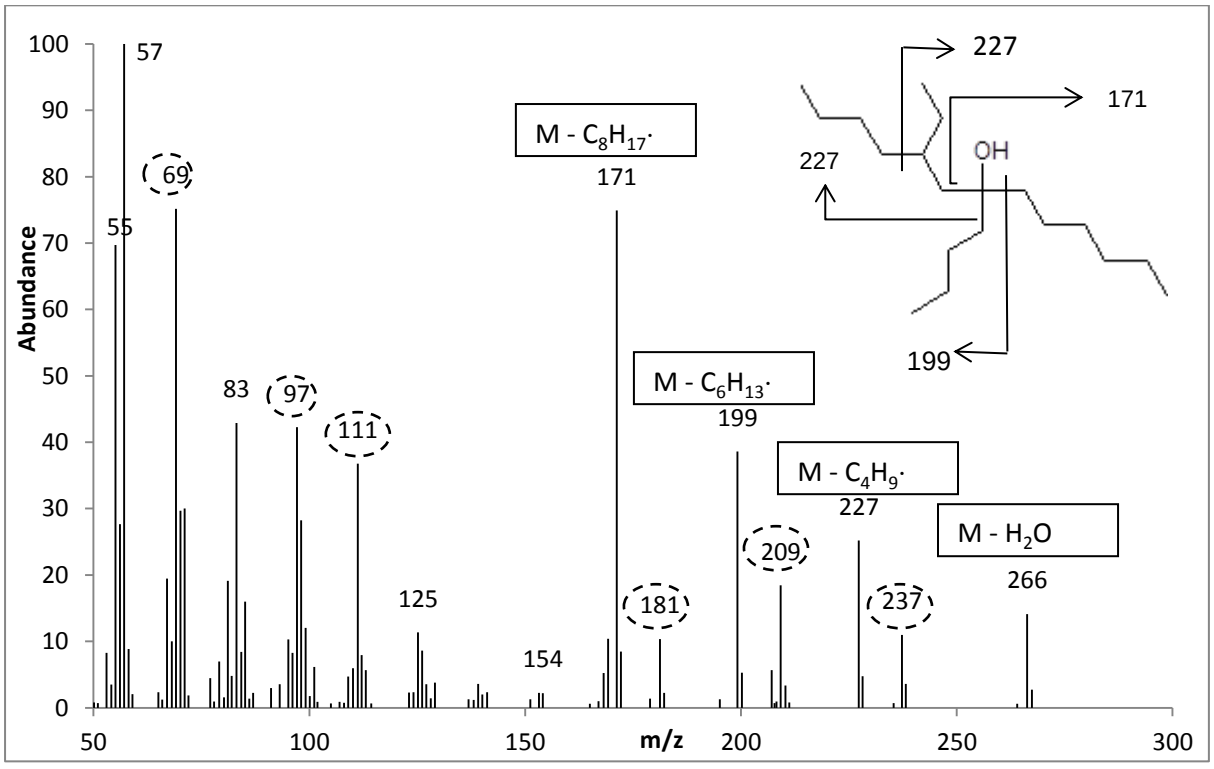

Figure 18: Mass spectrum of desired alcohol, 5-ethyl-7-butyltridecan-7-ol in crude product, indicates ion was from secondary fragmentation of dehydrated alcohol m/z 266

The mass spectrum of 5-ethyl-7-butyl tridecan-7-ol shows a complex fragmentation pattern because it contains two distinguishable low-mass ion series; some peaks originating from the molecular ion and some being a result of secondary fragmentation of the dehydrated alcohol. For example, the peaks at m/z 57 and 83 are low-mass ions indicative of saturated aliphatic hydrocarbons, fragmenting from the molecular ion ($M^{+\cdot}$ = 284). However the peaks at m/z 69, 97 and 111 are low-mass ions common to unsaturated aliphatics hydrocarbons (Smith, 2004). The peaks characteristic of the alcohol were m/z 266 which corresponds to the loss of water from the alcohol and the peaks at m/z 227, 199 and 171 represent α-cleavage at the tertiary carbons, seen in **Error! Reference source not found.** (McLafferty and Tureček, 1993).

The GC results of both syntheses showed a high abundance of remaining, unreacted 5-undecanone (**Figure 16** and **Figure 17**). The presence of ketone after the reaction and low yields suggest; either the Grignard reagent was low in concentration before the addition of the carbonyl, or the carbonyl and Grignard reagent underwent side reactions, not producing the desired alcohol. The results display evidence of side reactions during the formation of the Grignard reagent and during the Grignard reaction with the 5-undencanone.

The formation of the Grignard reagent, summarised in **Figure** below, is a complex mechanism involving single electron transfers (SET) and reactions between radicals.

$$\begin{aligned} R{-}X + \overline{Mg} &\longrightarrow R{-}X^{\bullet -} + Mg_s^{\bullet +} \\ R{-}X^{\bullet -} &\longrightarrow R^{\bullet} + X^{-} \\ X^{-} + Mg_s^{\bullet +} &\longrightarrow XMg_s^{\bullet} \\ R^{\bullet} + XMg_s^{\bullet} &\longrightarrow RMgX \end{aligned}$$

Figure 19: Supposed formation of Grignard reagent by SET and radical processes, $_s$ implies the reaction occurs at the surface of the metal (Smith and March, 2007)

The mechanism is only theoretical but based on empirical evidence such as trapping radicals in investigations. The reaction is known to occur on the surface of the metal and there arises the first possible problem during the reaction (Smith and March, 2007). If the magnesium turnings are not fresh and an oxide layer has formed, the reaction is limited by surface area of magnesium (Mayo *et al.*, 2000).

In the first synthesis, the reaction was initiated after scrapping and grinding the magnesium turnings with a glass rod, exposing the magnesium surface. The method worked but there are more effective ways to activate the metal surface using additional reagents, illustrated in the second synthesis which involved adding an iodine crystal. The iodine is believed to promote the reaction by reacting with the

magnesium to form a reactive MgI_2 salt, in turn removing the oxide layer exposing the metal surface (Kelly, 1998). The magnesium iodide formed is also thought to catalyse the reaction through a radical process and furthermore, magnesium iodide is hygroscopic therefore it will react with any water that is present before the Grignard reagent, removing another potential side reaction (Kelly, 1998, Sharma, 1998). Other methods involve preparation and use of Rieke's magnesium, for unstable Grignard reagents at low temperatures (Komiya, 1997).

The Grignard reagent is highly basic and will deprotonate any protic species such as water, resulting in the formation of an alkane e.g. 2-ethylhexane. The glassware was oven dried, a $CaCl_2$ guard tube was employed, sodium dried diethyl ether was used as the solvent and the system was closed to moisture when possible but without performing the reaction under inert conditions, even low moisture levels may have reduced the yield.

During the formation of the Grignard reagent, equilibrium is established between the Grignard reagent and by-products in a phenomenon known as the Schlenk equilibrium (Smith and March, 2007, Silverman and Rakita, 1996):

$$2\ R\text{-}MgX \rightleftharpoons R_2\text{-}Mg + MgX$$ (Smith and March, 2007)

In some solvents there is an additional step which involves the formation of dimers, $R_2Mg{\bullet}MgX$. However in THF and ether solvents, boiling point elevation and freezing point depression experiments have shown the products are all monomeric at low concentrations (Smith and March, 2007). The Schlenk equilibrium can be altered and is dependent on the alkyl bromide used, the concentration of the reagents and the temperature of the reaction.

During the syntheses, attempts to shift the Schlenk equilibrium to favour of the Grignard reagent included performing the reaction in large, dilute volumes of diethyl ether. Therefore newly formed Grignard reagent would be less likely to react with other Grignard reagent. Diethyl ether was chosen as the solvent because it is aprotic and the Grignard reagent has increased solubility in ether. The highly polarized C-Mg bond of the Grignard reagent means Grignard reagents are not generally soluble in non-polar organic solvents, with ether being the exception (Mayo *et al.*, 2000). The magnesium atom, within the Grignard reagent is Lewis acidic and the ether solvent is able to donate pairs of electrons to the electron deficient magnesium (Smith and March, 2007, Mayo *et al.*, 2000). The energy gained by two ether molecules coordinating with the Grignard reagent via the magnesium atom, increases the solubility of the Grignard reagent in ether (Mayo *et al.*, 2000). This association of ether with the Grignard reagent is important and another reason for using diluted volumes of starting reagents (**Figure**).

Despite ether being a good solvent for the Grignard reaction to proceed in, the products of the Schlenk equilibrium are also able to associate with the ether solvent (**Figure**). Canonne et al (1982) investigated the effects of different solvents during the reaction alkyl halides with diisopropyl ketone. The results showed that using benzene and toluene instead of ether and THF dramatically increased the nucleophilic addition products, reducing the side reactions (Canonne *et al.*, 1982).

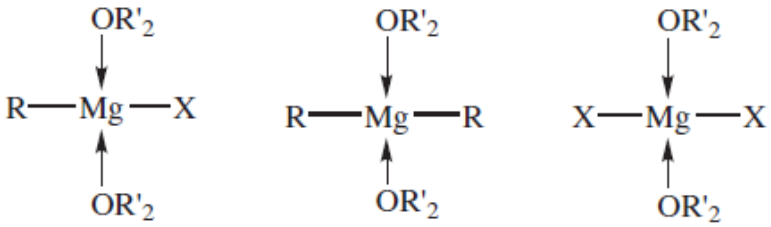

Figure 20: (a) Grignard reagent and (b) Schlenk products coordinate with the ether solvent resulting in enhanced solvation

The low yield and unreacted 5-undecanone are directly linked to the relatively high abundance of the peak at 13.9 min, identified as the Wurtz-type coupling product (**Figure 23**). The Wurtz-type coupling product is an additional step to the Schlenk equilibrium. The Grignard reagent will react with the alkyl halide, coupling the two alkyl groups forming an alkane and a magnesium salt:

$$R\text{-}MgX + R\text{-}X \longrightarrow R\text{-}R + MgX_2$$

The grey precipitate observed during the reaction is the formation of insoluble salts. The alkane was identified in the mass spectrum as the symmetric dimer 5,8-diethyldodecane (**Figure 22**).

To initiate the reaction in the first synthesis, several aliquots of alkyl halide were added alongside scrapping the magnesium turnings. If there is a high concentration of alkyl halide present during the initial formation of the Grignard reagent, it is more likely that the Grignard reagent will react with the alkyl halide forming the Wurtz-type coupling product before the addition of the ketone. Therefore, to improve the procedure in the second synthesis the addition of the alkyl halide was limited until the reaction had been initiated with the aid of an iodine crystal, enhancing the reactivity of the magnesium. Adapting the procedure was successful; the GC results showed a significant decrease in abundance from 19.5% to 12.8% of the Wurtz-type coupling product and the yield of 5-ethyl-7-butyltridecan-7-ol increased from 6.9% to 12.3%.

$M^{+\cdot} - C_6H_{13}\cdot$

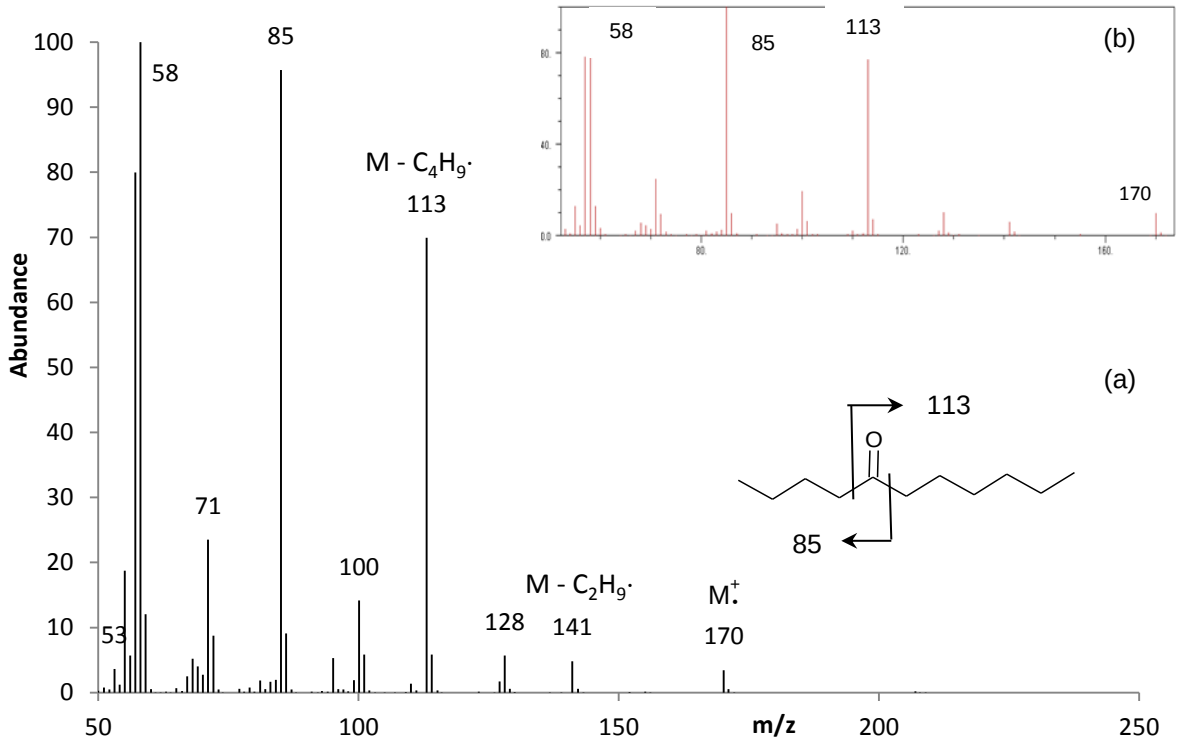

Figure 21: Mass spectrum of (a) 5-undecanone within crude product (b) library match from (Webbook, 2012)

The presence of unreacted 5-undecanone was confirmed by observations, IR and GC-MS. Firstly, the crude product had a very distinct pear/fruity aroma unique to 5-undecanone. The IR spectrum of the crude product showed a C=O stretch at 1712 cm^{-1} which matched the C=O stretch observed in the reference IR of 5-udencaone. The mass spectrum provided strong evidence for the fragmentation of 5-undecanone; the $M^{+\cdot}$ = m/z 170, the base peak at m/z 85 was a result from α-cleavage of the larger hexyl substituent and m/z 113 corresponded to α-cleavage of the smaller butyl group (**Figure**).

Additional evidence that the compound contained a carbonyl group was the appearance of even mass peaks at m/z = 58, m/z = 100 and m/z = 128. The occurrence of these peaks in a compound known to contain no nitrogen, with an odd-electron (OE^{+}) molecular ion suggests the even mass peaks correspond to rearrangement ions (Smith, 2004). If a compound contains a C=X, where X is a heteroatom or another carbon, and the compound contains a γ-hydrogen relative to double bond, it is able to undergo a γ-hydrogen rearrangement (Smith, 2004). When this occurs in a carbonyl compound, the phenomenon is known as the McLafferty rearrangement (Smith, 2004, McLafferty and Tureček, 1993).

The peak at m/z = 128 would result from the rearrangement involving the γ-hydrogen of the butyl substituent. The peak at m/z = 100 would result from the rearrangement involving the γ-hydrogen of the hexyl group. The m/z = 58 could correspond to a CH2=C(OH+)CH3 structure possibly produced from the secondary fragmentation of a rearrangement ion or from a double McLafferty rearrangement (Smith, 2004).

The predicted structure of the Wurtz-type coupling product was 5,8-diethyldodecane, supported by the mass spectrum showing a peak accounting for the molecular ion at $M^{+\cdot}$ = m/z 226 (Figure **22**22). The mass spectrum showed a typical low-mass ion series of a branched aliphatic hydrocarbon i.e. with peaks at m/z = 57, 71, 85. Aliphatic hydrocarbons often show characteristic losses representing the fragmentation of alkyl groups such as butyl, pentyl and hexyl fragments. These losses were identified in Figure 22 as peaks at m/z 169, 155 and 141. The low mass ions usually have a higher abundance, decreasing almost exponentially towards the molecular ion peak, again observed in Figure **22**22.

The structure of 5,8-diethyldodecane is symmetrical and the peak at m/z 113 corresponds to fragmentation of the central bond between the two α-carbons adjoining the two tertiary carbons (Figure **22**22).

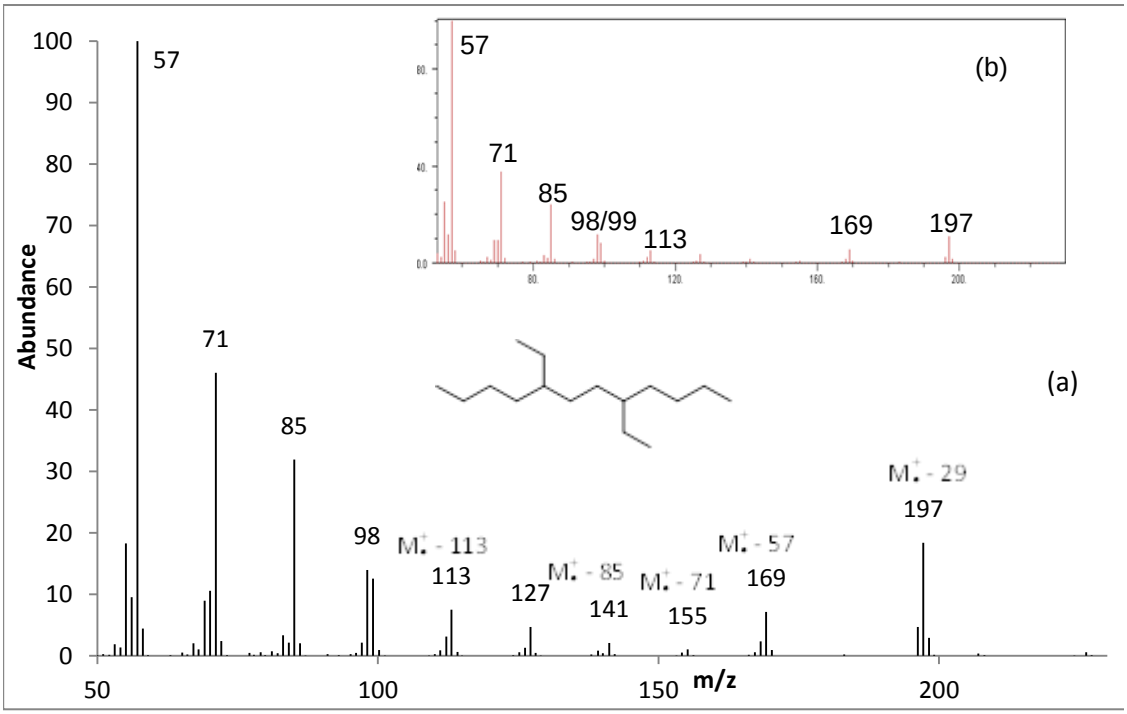

Figure 22: Mass spectrum of (a) Wurtz-type coupling compound identified in crude product and (b) library match of 5,8-diethyldodecane (Webbook, 2012)

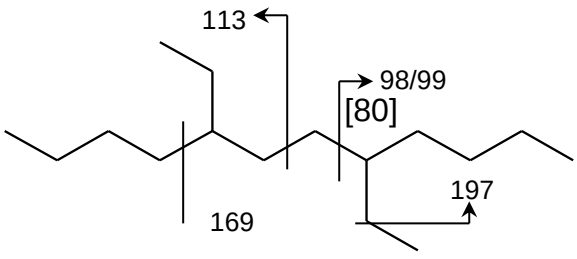

Figure 23: Structure and fragmentation of the Wurtz-type coupling product; 5,8-diethyl dodecane

The mass spectrum of the Wurtz-type coupling product was compared with a library search of 5,8-diethyldodecane and the two spectra matched identically (Figure **22**22). An unusual however key feature confirming the structure of the by-product was the pair of peaks at m/z 98 and 99. McCarthy et al (1968) discovered, after investigating several mass spectra from the American Petroleum Institute (API), that saturated aliphatic hydrocarbons show the appearance of a C_nH_{2n} even mass ion, alongside the C_nH_{2n+1} ion. This occurs when straight chains containing seven or more carbons fragment. The even-mass ion is due to a hydrogen transfer during the α-cleavage at a tertiary carbon (McCarthy *et al.*, 1968). If the fragment contains no branching, the even-mass ion has a greater abundance than the odd mass ion and this phenomenon is observed for mono- and dialkyl branched hydrocarbons except dialkyl hydrocarbons with the substituents on the same carbon (McCarthy *et al.*, 1968). In Figure 22, the peak at m/z 98 was greater than the m/z 99 ion because 5,8-diethyldodecane can fragment at a tertiary carbon resulting in a straight chain ion, seven carbons long (Figure **23**23). Included in their investigation, McCarthy et al (1968) analysed 5,8-diethyldodecane and the mass spectra contained a pair of peaks at m/z 98 and 99 with the m/z 98 ion in with a higher intensity.

The occurrence of even-mass ions, resulting from a hydrogen transfer has been recorded in several investigations including the analysis of insect lipids and HBIs, during the identification of dialkyl branched, long chain aliphatic hydrocarbons using GC-MS (Kenig *et al.*, 1995, Nelson and Sukkestad, 1970).

3.3 Purification of Crude Product

The crude product required purification before proceeding to the dehydration of the tertiary alcohol. The crude product contained by-products of the Grignard reaction such as the Wurtz-type coupling product and unreacted starting materials such as 5-undecanone. Column chromatography was performed to separate, at least the polar from the non-polar compounds. The complete separation of the alcohol from the ketone was unfeasible due to the similar polarities, however a mixture the ketone and alcohol together was considered adequate separation as the ketone would not have affected the remaining dehydration and hydrogenation stages.

Gravimetric analysis was performed throughout the column chromatography which involved removing the solvent by nitrogen blow down and recording the accurate mass of each fraction. The mass of each fraction was then plotted as a preliminary chromatogram, indicating the elution of a compound (**Error! Reference source not found.**

Figure24).

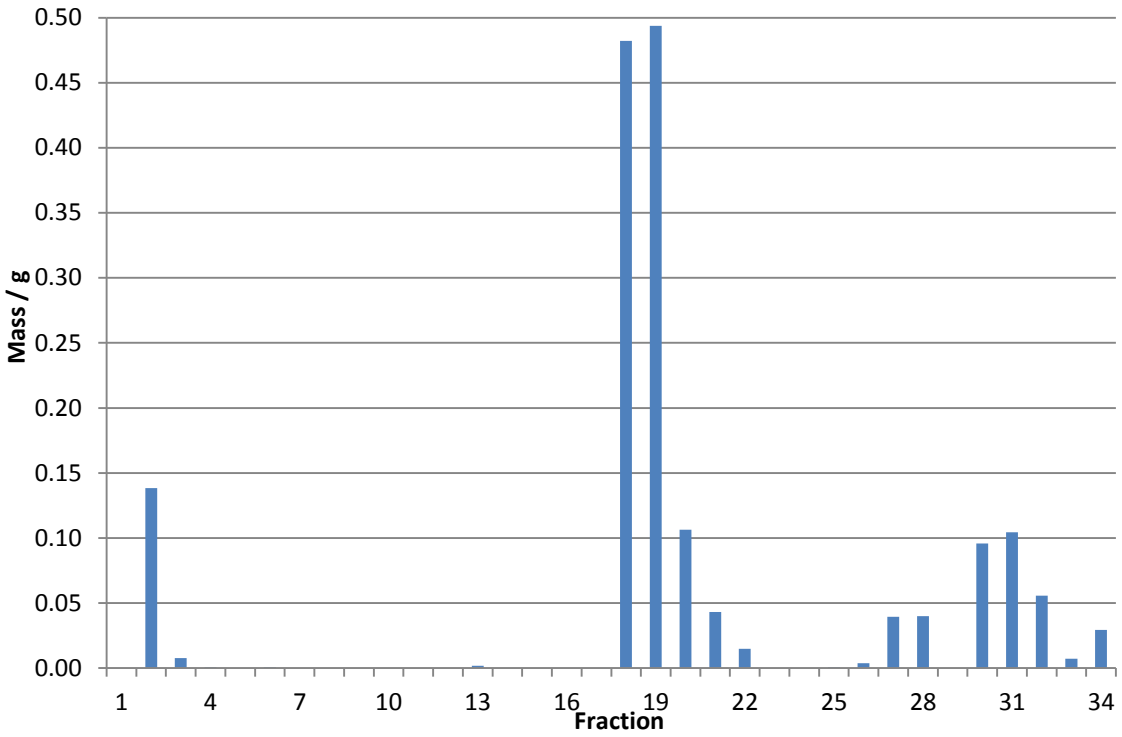

Figure 24: Chromatogram plotted using the mass of each fraction

Figure24 shows the elution of a non-polar compound across fractions 2 and 3, initially thought to be the Wurtz-type coupling product. Next followed the elution of more polar compounds in fractions 18-22; **Error! Reference source not found.** the eluate tailed across 6 fractions indicating the possible staggered, co-elution of the ketone and alcohol. The dot test of fractions 18-20 under a UV light showed fluorescence and the fractions also smelt of 5-undecanone. Fractions 26-28 and 30-34 showed the elution of the most polar compounds eluting in 50% and 100% diethyl ether and finally methanol. These were likely to represent impurities in the crude product, alongside water removed from the silica stationary phase. To identify the compounds that separated, GC-MS was performed on only selected fractions which would represent the elution of different compounds observed.

GC-MS of fraction 2 confirmed that it was the isolated Wurtz-type coupling product (**Figure**25). The high purity (98.2%) of 5,8-diethyldodecane illustrated the high level of separation that could be achieved using column chromatography.

Fraction 2 was identified as 5, 8 diethyl dodecane by comparison of the retention times of the peak with the peak in the crude product, 12:22 min and 12:18 min respectively. To confirm its structure the mass spectra of the two peaks were also compared and were identical, as shown in **Figure**25.

The GC results of fractions 18-21 showed the elution of 5-undecanone followed by the elution of the product, 5-ethyl-7-butyltridecan-7-ol. The compounds were identified by comparing the mass spectra with the mass spectra of the compounds within the crude product. A peak for the alcohol was not observed due to dehydration

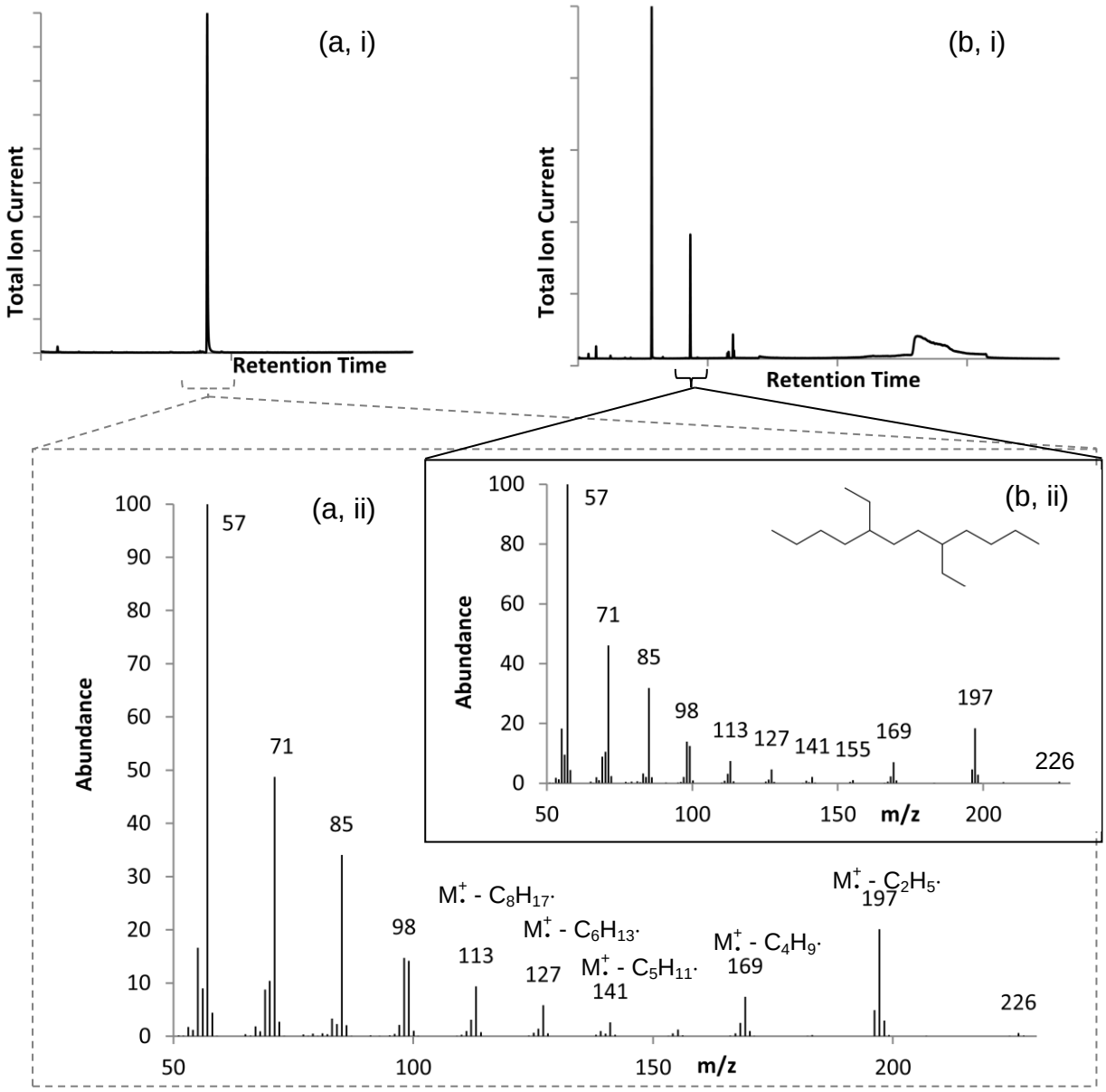

Figure 25: (a, i) GC of Fraction 2 and (a, ii) mass spectrum of Fraction 2 compared with (b, i) GC of crude product and (b, ii) mass spectrum of 5, 8 diethyl dodecane

during GC-MS, however the separation of the alcohol was indicated by the presence of four distinct peaks representing the alkene isomers of the dehydrated alcohol.

There was some overlap during the elution of the two compounds as expected because the compounds have similar polarities; the relative quantity of 5-undecanone decreased and the quantity of alcohol increased as the number of fractions increased (**Table 1**). This demonstrates that the ketone eluted slightly before the alcohol; the staggered co-elution is displayed in (**Figure**26 and **Figure**27). The slight separation between two compounds shows the chromatographic technique was effective but still did not provide a pure sample of the product.

Table 1: Relative quantities of ketone and product eluting in fractions 18-21, showing staggered co-elution

Fractions	Mass / g	Relative Quantity / %	
		5-undecanone	5-ethyl-7-butyl tridecan-7-ol
18	0.4822	91.4	8.6
19	0.4937	83.4	15.3
20	0.1064	38.6	61.1
21	0.0432	8.4	91.6

The GC results of fractions 20 and 21 contained the highest, purest quantity of the desired 5-ethyl-7-butyltridecan-7-ol. Therefore fractions 20 and 21 were combined and used to proceed with the dehydration stage.

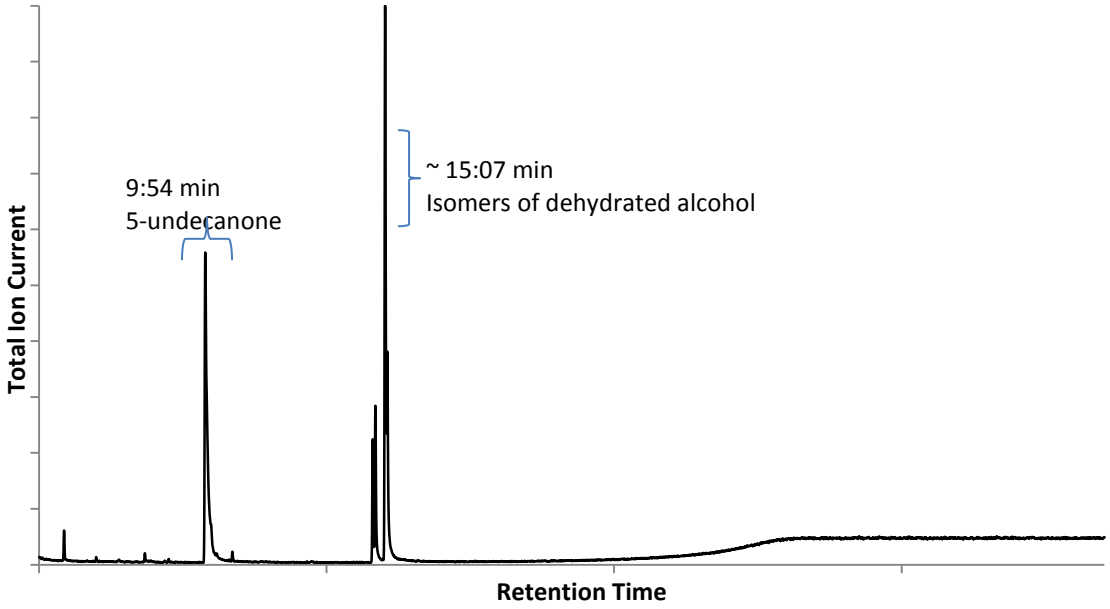

Figure 26: Gas chromatogram of fraction 20 showing the relative intensities of 5-undecanone and 5-ethyl-7-butyltridecane isolated by column chromatography

The GC results of fractions 20 and 21 contained the highest, purest quantity of the desired 5-ethyl-7-butyltridecan-7-ol. Therefore fractions 20 and 21 were combined and used to proceed with the dehydration stage.

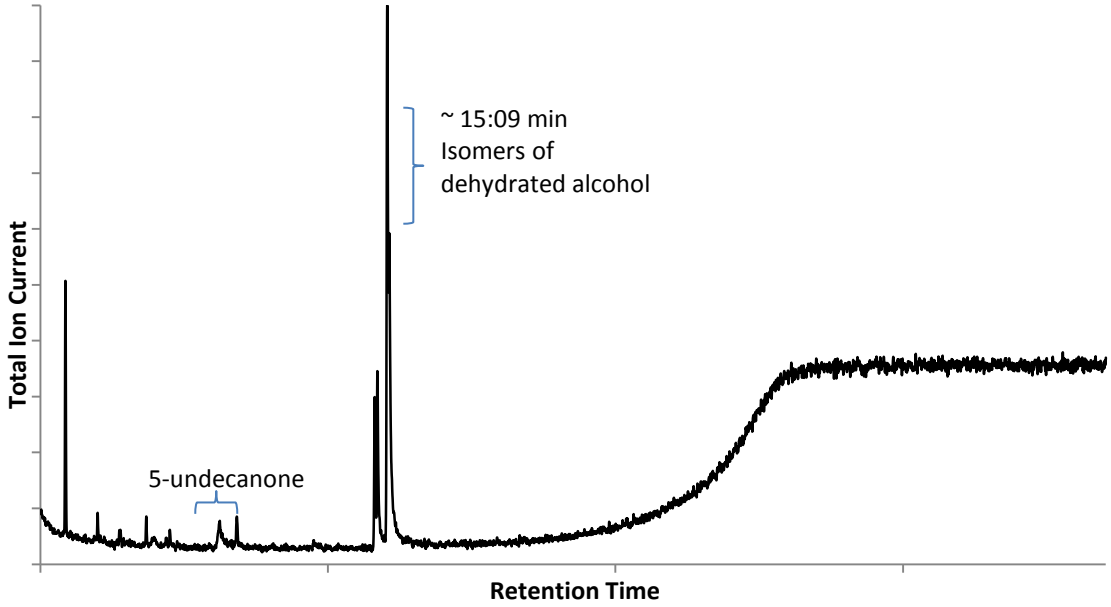

Figure 27: Gas chromatogram of fraction 21 showing the relative intensities of 5-undecanone and 5-ethyl-7-butyltridecane isolated by column chromatography

3.4 Synthesis of 5-ethyl-7-butyltridecene

The low quantity of product obtained by combining fractions 20 and 21, isolated using column chromatography, meant particular care was required during the remaining dehydration and hydrogenation steps. Therefore a practice dehydration was performed on n-dodecanol to gain experience using low quantities of product, which showed a high recovery (70%) was achievable. The procedure used $POCl_3$ as it is effective for dehydrating tertiary alcohols (Smith, 2011). The reaction scheme shows resonant bonds about the tertiary carbon because the dehydration produced a series of alkene isomers (

Figure28).

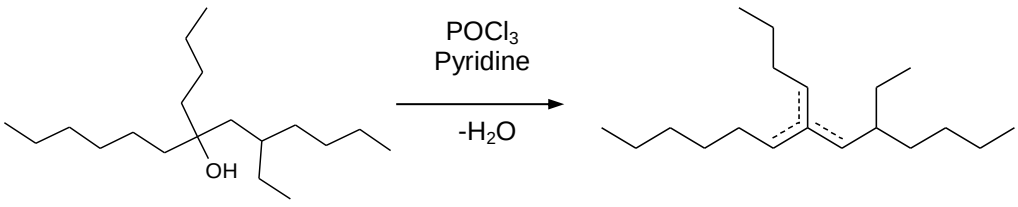

Figure 28: Reaction scheme for the dehydration and synthesis of 5-ethyl-7-butyltridecene

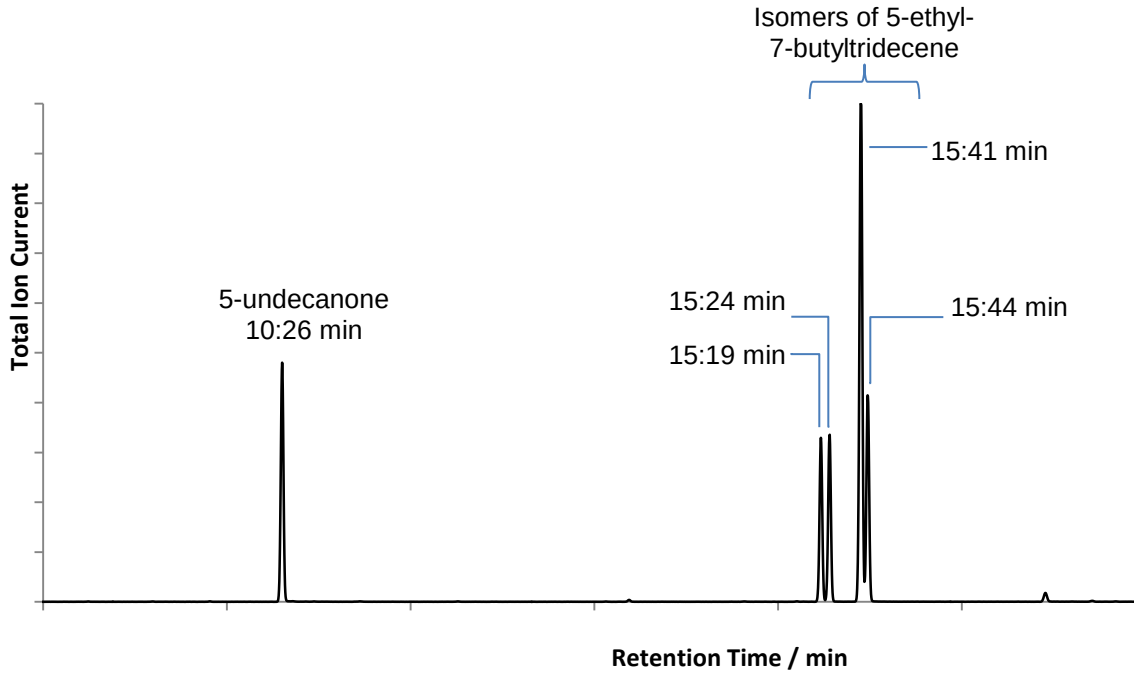

Figure 29: Gas chromatogram of dehydration product

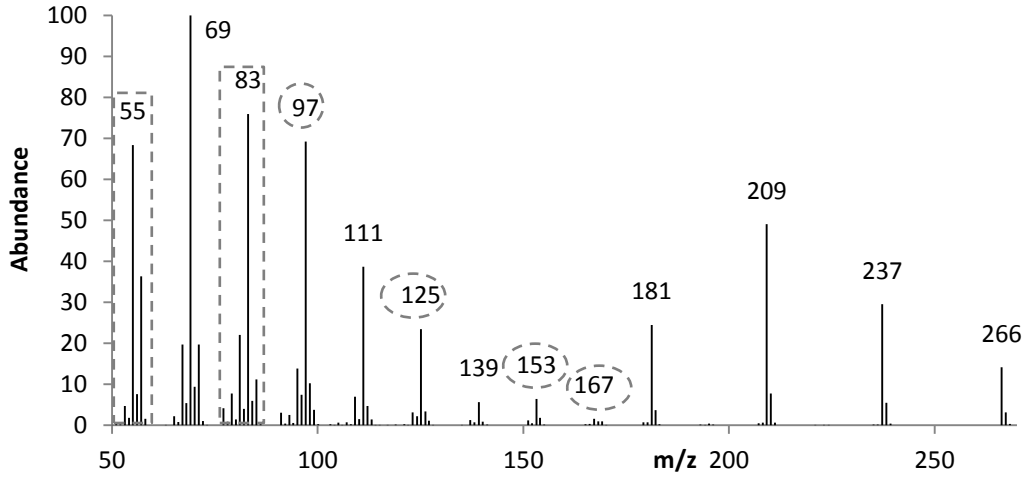

Figure 30: Mass spectrum of the peak at 15:24 min; isomer of 5-ethyl-7-butyltridecene

Figure29 shows a peak with a retention of 10:26 min, with a mass spectrum that was an identical match of 5-undecanone. This accounted for the small quantity of ketone in the sample due incomplete separation during column chromatography.

The gas chromatogram showed four peaks observed at 15:19, 15:24, 15:41 and 15:44 min, thought to be the isomers of 5-ethyl-7-butyltridecene. The retention times of the four peaks did not match those previously seen in the GC of the tertiary

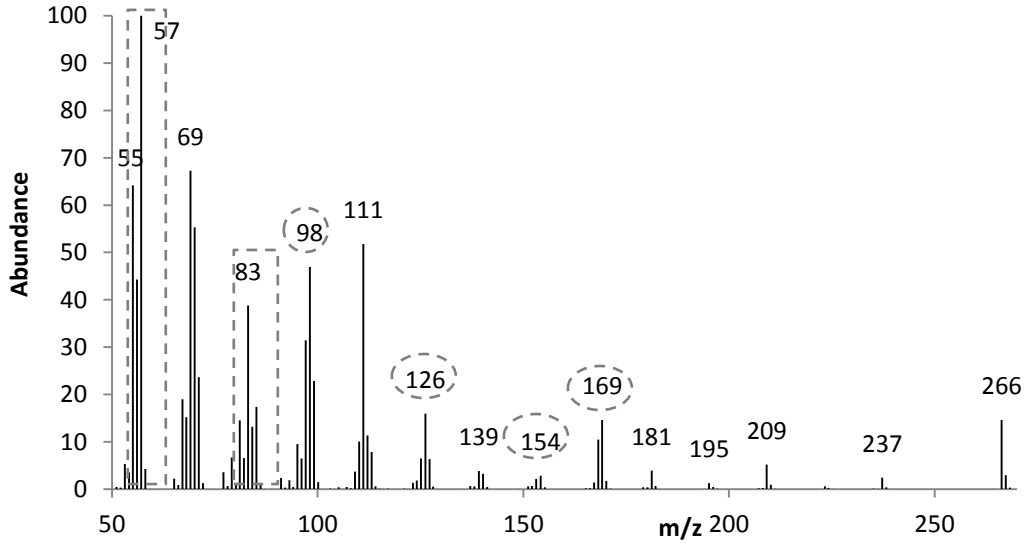

Figure 31: Mass spectrum of the peak at 15:41 min; isomer of 5-ethyl-7-butyltridecene

alcohol, observed due to the dehydration of the alcohol within the GC column. However the peak separation i.e. the retention time of each peak relative to the following peak was the same. The retention time of a compound can vary with conditions and over time with the age and maintenance of the column. However the elution order of the isomers, the abundance and the retention times relative to the 5-undecanone peak remained the same.

Therefore the appearance of the four peaks, the relative retention times and the disappearance of the alcohol peak at a longer retention time, indicated a successful dehydration.

The mass spectra provided further evidence confirming the synthesis of the alkenes. The four peaks eluted as two pairs and the pair that eluted at 15:19 and 15:24 min had very similar mass spectra, represented in **Error! Reference source not found.**30. The second pair of peaks that eluted after also had similar mass spectra, represented in **Figure**31. However, when comparing the mass spectra of the two pairs there were slight variations, suggesting structural differences, highlighted in **Error! Reference source not found.** and 31.

The most commonly ionised position of an alkene is the carbon-carbon double bond (Dass, 2007). This results in an odd-electron molecular ion, $M^{+\cdot}$ seen in the mass spectra as the peak at m/z 266. Molecular ions of alkenes typically have a low abundance as they are relatively unstable (Gross, 2011). The double bond is able to migrate within the compound and can result in allylic-cleavage. Alkenes can also undergo a γ-hydrogen rearrangement, similar to the McLafferty rearrangement (Dass, 2007). Consequently, the mass spectra of isomeric alkenes are structurally

indifferent and using mass spectra alone means the isomers are indistinguishable due to the mobility and fragmentation (Dass, 2007).

Despite the ambiguity in the identification of isomeric alkenes, the appearance of certain peaks in the mass spectra can be accounted for and give an insight into the types of fragmentation observed. **Error! Reference source not found.**30 and 31 show low-mass ion series, characteristic of unsaturated aliphatic hydrocarbons such as C_nH_{2n-1} ions, e.g. m/z 55, 69, 83 (**Error! Reference source not found.** and 31), 97 and 111 (**Error! Reference source not found.**30) and C_nH_{2n} ions e.g. m/z 98 and 226 (Figure31) (Smith, 2004).

The peaks at m/z 237 and 209 are indicative of allylic-cleavage, accounting for the loss of an ethyl and butyl group, respectively. An allylic-cleavage occurs when a radical site produced during ionisation produce the fragmentation of alkene radical cations; the cation is then able to isomerise (Dass, 2007).

The double bond within the isomers of 5-ethyl-7-butyltridecene includes a tertiary carbon. Therefore ionisation of the double bond would result in the positive charge residing on the tertiary carbon due to an increased stability, meaning the allylic-cleavage would occur at the α-carbons. A possible example of allylic-cleavage occurring in an isomer of 5-ethyl-7-butyltridecene is given in **Error! Reference source not found.**32, resulting in a peak at m/z 237 and the formation of a low-mass ion at m/z 97 due to secondary fragmentation, two ions both seen in **Error! Reference source not found.**30.

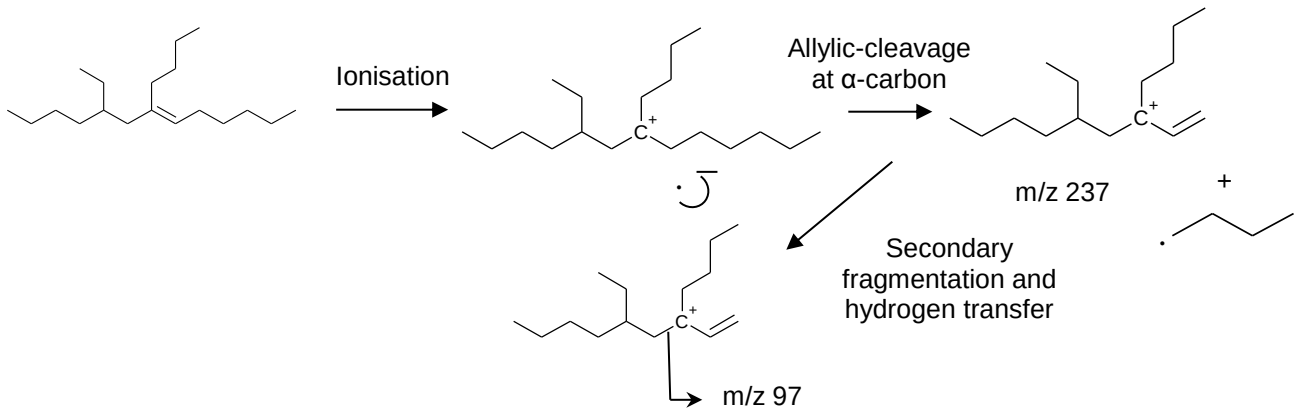

Figure 32: Mass spectrum of the peak at 15:41 min; isomer of 5-ethyl-7-butyltridecene

The alkenes can show stereoisomerism displayed as E/Z isomers about the C=C bond. The presence of only four peaks shows not all the isomers were co-elute but as there are more than four isomers this shows some must co-elute, possibly one form of an isomer e.g. E, co-eluting with the Z conformation of another isomer. The mass spectra only vary slightly as the alkene isomers have very similar structures.

3.5 Synthesis of 5-ethyl-7-butyltridecane

The dehydration produced a mixture of 5-ethyl-7-butyltridecene isomers. To synthesis 5-ethyl-7-butyltridecane, the product was diluted in 50% ethyl acetate/hexane and hydrogenated by bubbling hydrogen through the solution in the presence of a 10% palladium on carbon catalyst. The reaction mixture was left hydrogenating for 6 hours in an attempt to completely convert the entire product to the saturated alkane (**Figure 33**33).

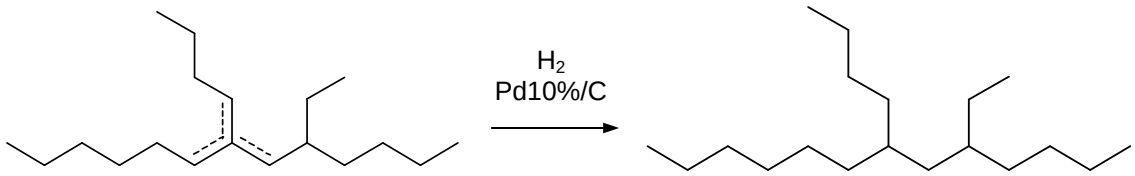

Figure 33: Reaction scheme of hydrogenation in the synthesis of 5-ethyl-7-butyltridecane

The reaction produced a reasonable yield of 58% and a high purity of 81.2%. The product was analysed by GC-FID and GC-MS.

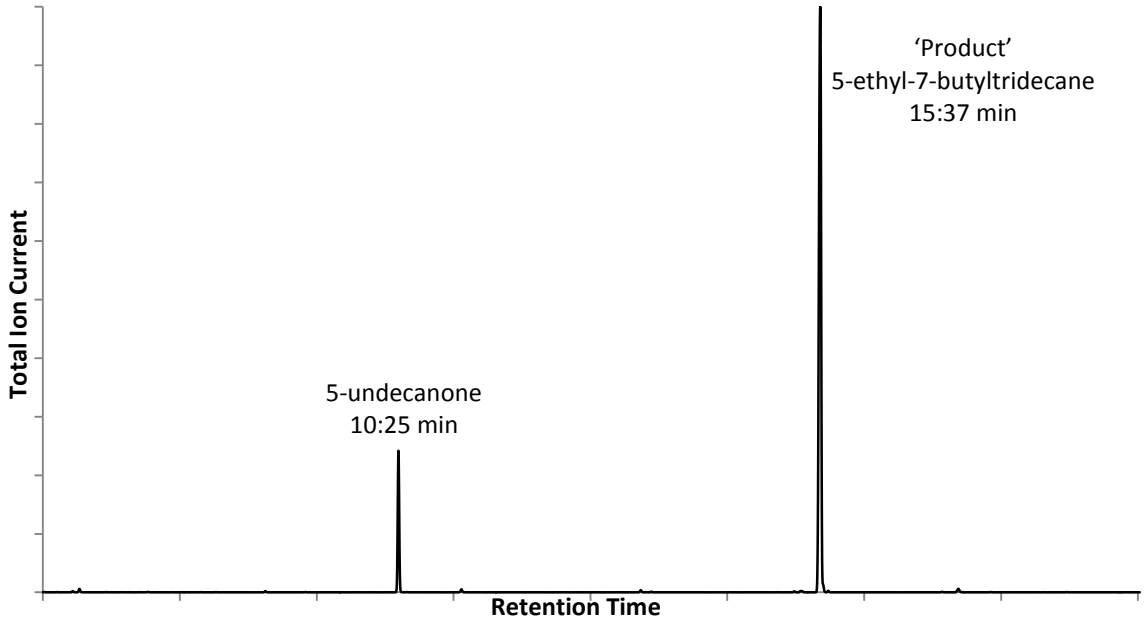

Figure 34: Gas chromatogram of hydrogenated product

The gas chromatogram of the hydrogenated product showed two peaks (**Figure 34**34). The elution at 10:25 min was identified as 5-undecanone, present in the mixture of alkenes, originating from the incomplete separation of the tertiary alcohol and ketone during column chromatography. The structure was confirmed by its mass spectrum.

The disappearance of the four peaks, ranging from 15:19 min to 15:44 min and appearance of a single peak with a retention time within the range at 15:37 min, suggests the hydrogenation was successful in hydrogenating the mixture of isomeric alkenes to a single alkane. The similarity in retention times indicates the structure and polarity of the product was very similar to alkenes, as expected.

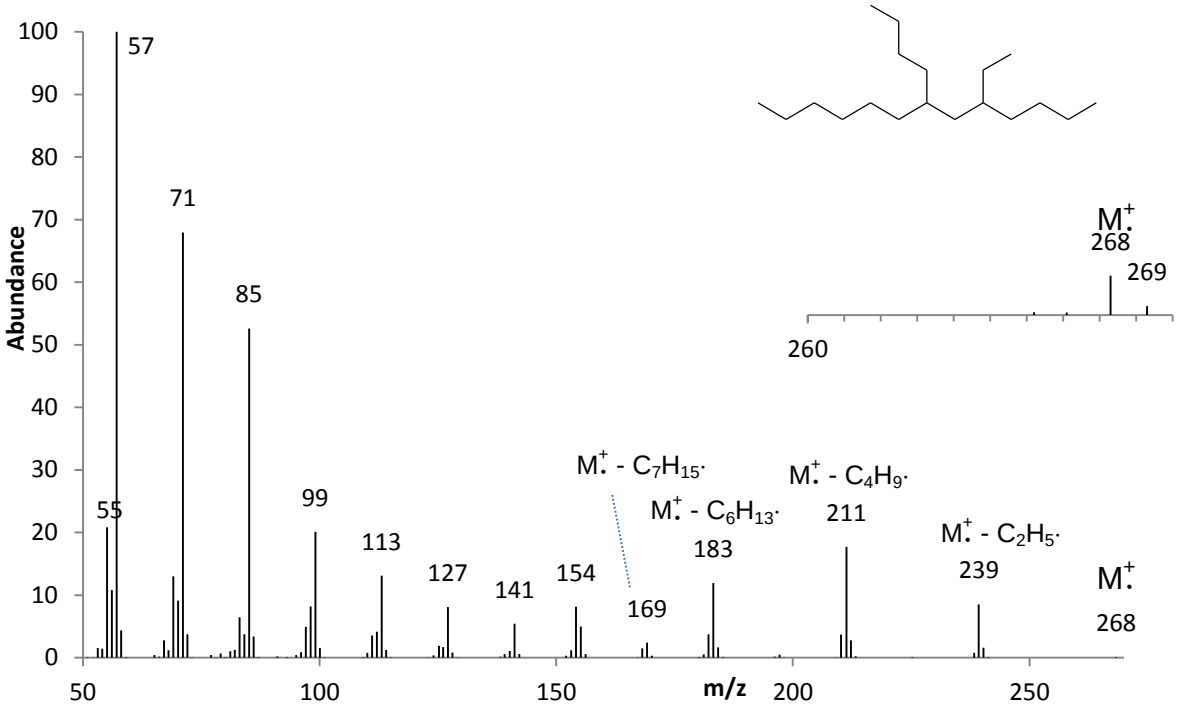

Figure 35: Mass spectrum of hydrogenated product; 5-ethyl-7-butyltridecane

The mass spectrum of the peak which eluted at 15:37 min displayed a molecular ion at $M^{+\cdot}$ = m/z 268, corresponding to a $C_{19}H_{40}^{+\cdot}$ structure. Further evidence to suggest the compound contained 19 carbon atoms is that ratio between the abundance of m/z 268 (0.13 abundance) and 269 (0.03 abundance) was equal to natural isotopic ratio of ^{12}C to ^{13}C. The natural abundance of ^{13}C is 1.1% (McLafferty and Tureček, 1993).

$$((0.03 / 0.13) / 19) \times 100 = 1.2\%$$

Figure 3535 shows a typical low-mass C_nH_{2n+1} ion series, indicative of a saturated hydrocarbon, with peaks at m/z 57, 71, 85 and 99. The high abundances of the low-mass ions decreases almost exponentially towards the high mass ions, which is another characteristic of branched alkanes (Smith, 2004).

The higher mass ions gave more structural detail, confirming the positions of the tertiary carbons. Fragmentation occurs at the α-carbons of the tertiary centres via α-cleavage. Ionisation at the tertiary carbon is encouraged by the steric interactions between the large alkyl substituents, weakening of the bonds meaning they are more likely to be ionised and fragment. The positive charge then resides on the tertiary carbon and this is the fragment detected. Therefore, the peaks at m/z 239, 211 and 183 correspond to the loss of an ethyl ($M^{+\cdot}$ - 29), butyl ($M^{+\cdot}$ - 57) and hexyl ($M^{+\cdot}$ - 85) group, respectively, all present in 5-ethyl-7-butyltridecane.

The increased intensity of the peak at m/z 211 ($M^{+\cdot}$ - $C_4H_9\cdot$), compared to m/z 239 ($M^{+\cdot}$ - $C_2H_5\cdot$) and m/z 183 ($M^{+\cdot}$ - $C_6H_{13}\cdot$) suggests that there are two butyl groups attached to tertiary carbons and only one ethyl and one hexyl group which matches the structure of 5-ethyl-7-butyltridecane.

The peak at m/z 169 relates to the loss of a heptyl group ($M^{+\cdot}$ - 99), resulting from α-cleavage between carbons 5 and 6 (**Figure 36**36). The pair of peaks at m/z 154 and 155 has been identified by Kenig et al (2005) as diagnostic peaks for butyl-ethylalkanes. They proposed the doublet occurs due to the neutral loss of an n-alkyl fragment with an even number of carbons (Kenig *et al.*, 2005). This would occur in 5-ethyl-7-butyltridecane due to the fragmentation between carbons 6 and 7 by α-cleavage at a tertiary carbon, resulting in a $C_{11}H_{23}^{+}$ m/z 155 ($M^{+\cdot}$ - 113), corresponding to the loss of an even number $C_8H_{17}\cdot$ neutral radical. The peak at m/z 154 could also be a result of a hydrogen rearrangement during the fragmentation process.

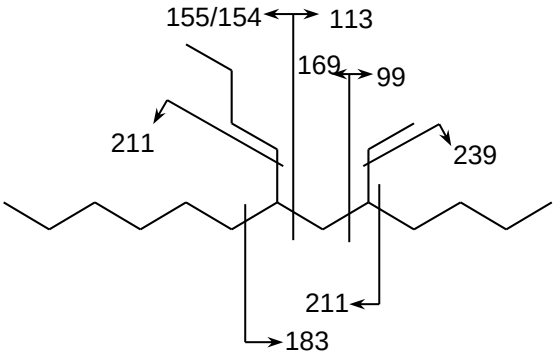

Figure 36: Fragmentation by α-cleavage at the tertiary centres, confirming the synthesis of 5-ethyl-7-butyltridecane

The observation of pair of peaks, characteristic to the position of the branching within alkane was seen previously in the mass spectrum of the Wurtz-type coupling product, 5,8-diethyldodecane (**Figure 22**22). However the pair of peaks at m/z 98 and 99 provided no diagnostic evidence for the structure of 5-ethyl-7-butylridecane, despite 5-ethyl-7-butyltridecane being able to undergo the same α-cleavage between carbons 5 and 6 producing a $C_7H_{13}^{+}$ (**Figure 35**35). The intensity of the peaks at m/z 98 and 99 were much less similar, compared with the intensities seen in **Figure 22**22. This could be due to 5-ethyl-7-butyltridecane fragmenting into more, larger fragments, producing higher mass ions which then underwent secondary

fragmentation resulting in a $C_7H_{13}^+$ ion. This would increase the intensity of the peak m/z 99 alone, altering the ratio between m/z 98 and 99. A different reason may be due to the two tertiary carbons being closer together in 5-ethyl-7-butyltridecane compared with 5,8-diethyldodecane. The decreased distance between the two alkyl branches may have affected the fragmentation of the α-cleavage between carbons 5 and 6, possibly steric effects promoting the loss of the C_nH_{2n+1} ion, m/z 99 over the loss of the C_nH_{2n} ion, m/z 98.

The results of the GC and mass spectrum showed strong, comprehensive evidence that the synthesis of 5-ethyl-7-butyltridecane was successful.

3.6 Chromatographic Effects of H-branch Alkanes and Various Isomers

The gas chromatogram of 5-ethyl-7-butyltridecane showed a single peak suggesting a single isomer. The structure of 5-ethyl-7-butyltridecane, containing two stereogenic carbons, shows four possible conformational isomers. These correspond to two pairs of enantiomers i.e. mirror images, which are diastereoisomers of each other i.e. not mirror images (Clayden *et al.*, 2001). The two stereogenic carbons can each show R/S stereoisomerism. The chiral carbons can show R/R and S/S which are a pair of enantiomers and the corresponding diastereoisomers; R/S and S/R which are a different pair of enantiomers (Figure37).

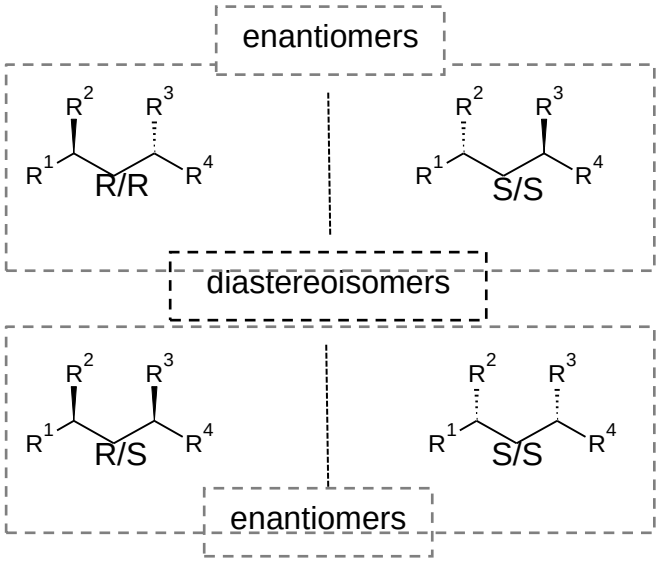

When $R^1 = C_4H_9$ $R^2 = C_2H_5$ $R^3 = C_4H_9$ $R^4 = C_6H_{13}$

Figure 37: Stereoisomerism shown by 5-ethyl-7-butyltridecane

In a gas chromatogram enantiomers often co-elute, unless a chiral stationary phase is employed or GC×GC. They have the same physical properties and as a result have the same boiling points and retention times. Conversely, diastereoisomers are distinguishable in gas chromatograms but the separation is dependent on the resolving power of the GC and also for H-branch alkanes, the similarity of the of the alkyl branches on carbon 7 of the linear backbone.

There was no appearance of two peaks in the GC and GC-MS of 5-ethyl-7-butyltridecane, so the temperature programme was adapted in an attempt to increase the separation of the diastereoisomers. The temperature programme was changed from 40-300 °C at 10 °C min^{-1} to 40 -300 °C at 5 °C min^{-1}, held for 20 min.

Samples of 5-ethyl-7-pentyldodecane and 5-ethyl-7-propyltetradecane i.e. other H-branch alkanes, were also analysed by GC-MS to compare the effects of the H-branch structure on the resolution of diastereoisomers.

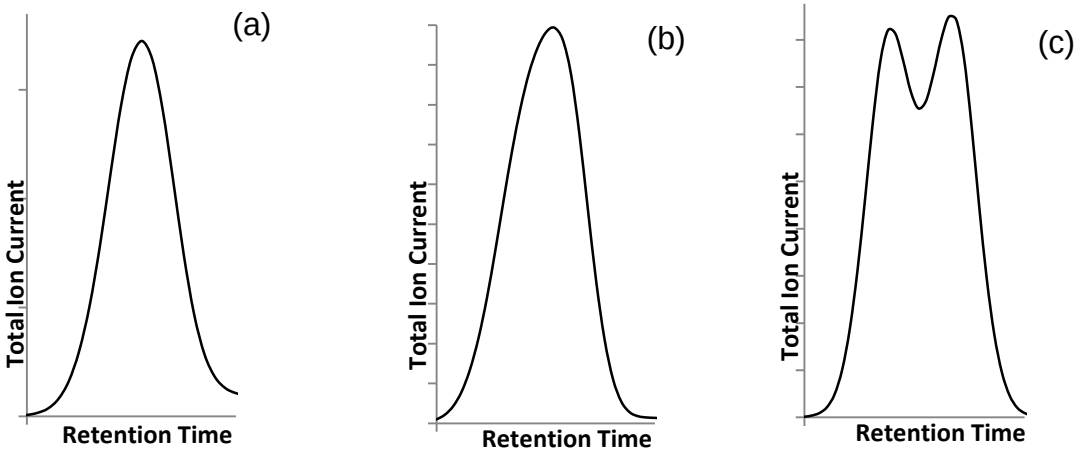

Figure 38: Comparison of (a) 5-ethyl-7-pentyldodecane, (b) 5-ethyl-7-butyltridecane and (c) 5-ethyl-7-propyltetradecane gas chromatograms

The GC of 5-ethyl-7-pentyldodecane only showed one peak (Figure38a), with a typical Gaussian shape because it only contains one stereogenic centre; two of the alkyl substituents of the same tertiary carbon are both pentyl groups, therefore the carbon is not stereogenic (Figure39a). The GC of 5-ethyl-7-butyltridecane still did not show two peaks for the adapted temperature programme. However the peak does show slight distortion and leaning suggesting the co-elution of the diastereoisomers (Figure38b). The alkyl groups on carbon 7 are a butyl and hexyl group, very similar in length (Figure39b). The GC of 5-ethyl-7-propyltetradecane shows slight separation of the diastereoisomers; they are not fully resolved but there is definite evidence of two compounds with very similar retention times, hence similar structures i.e. diastereoisomers (Figure38c). The alkyl groups on carbon 7 show more variation with a propyl and heptyl group, corresponding to a more significant difference in structure (Figure39c).

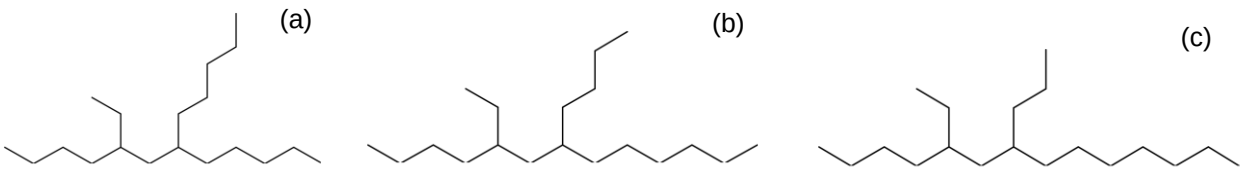

Figure 39: (a) 5-ethyl-7-pentyldodecane, (b) 5-ethyl-7-butyltridecane and (c) 5-ethyl-7-propyltetradecane

The GC results of 5,7-diethylpentadecane and 5-ethyl-7-methylhexadecane were also analysed. A trend was observed throughout the H-branch series; as the alkyl substituent on carbon 7 decreases in carbon number and the length of the main chain increases in carbon number, the resolution between the diastereoisomers increases and they become almost completely separated as the difference in structure increases.

Furthermore, the retention time of H-branch alkanes was seen increasing as the alkyl substituent on carbon 7 decreases in length and the main chain increases in length. This trend was similar to that observed in the investigation of C_{19} T-branch alkanes; the ethyl-heptadecanes had the highest retention indices and the hexyl-tridecane i.e. all three alkyl groups being the same, had the lowest retention index (Figure40). To compare the elution order of the H-branch alkanes and how the retention times compare with the T-branch alkanes, the retention index of the three H-branch alkanes analysed by GC, were calculated and shown in (Figure40) (Sparkman *et al.*, 2011).

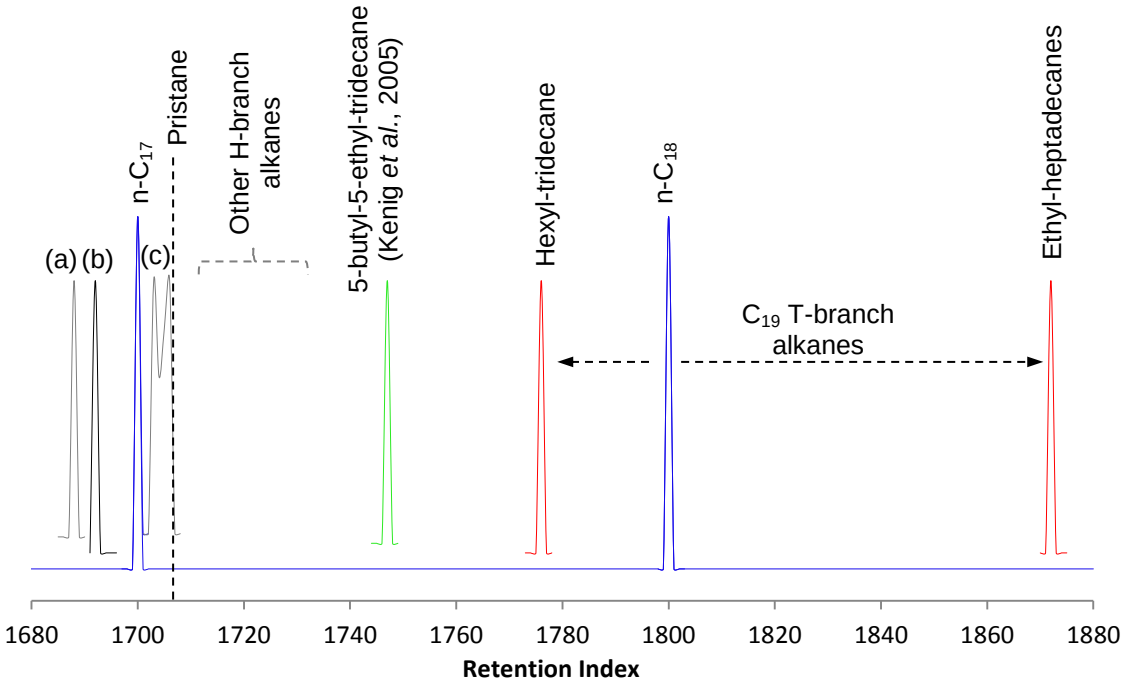

(a) 5-ethyl-7-pentyldodecane, (b) 5-ethyl-7-butyltridecane and (c) 5-ethyl-7-propyltetradecane representing H-branch alkanes, compared with pristane (RRI 1707), 5-butyl-5-ethyltridecane and the T-branch alkane series. Retention index for HP-5MS capillary column, calculated from retention times relative to n-heptadecane and n-octadecane.

Figure 40: Retention index comparing H-branch alkanes, T-branch alkanes and various C_{19} branched isomers

Figure40 shows that an increase in branching reduces the retention time of a compound, to such an extent that C_{19} H-branch alkanes elute in a similar time of a C_{17} straight chain alkane. This effect is common and could be a result of branching, reducing the strength of the interactions with the stationary phase within the GC column or reducing interactions between molecules, therefore lowering the boiling point and retention time (Crippen, 1973). The two H-branch alkanes most recently synthesised, 5-ethyl-7-pentyldodecane and 5-ethyl-7-butyltridecane, surprisingly elute before *n*-heptadecane, at 1688 and 1692 Kovats, respectively (**Figure**40). Prior to this investigation, pristane was thought to be the earliest eluting branched C_{19} compound, with a retention index of 1707 Kovats as the results observed by Lewis *et al.* (2009) showed the T-branch alkanes eluting significantly later between1872-1776 Kovats (**Figure**40).

It would appear that the position of the alkyl branching also has an effect on the retention time. The 5-butyl-5-ethyl-tridecane, identified in Cenomanian black shales in Pasquia Hills, Canada by Kenig et al (2005) had a retention index 55 Kovats higher than the product synthesised in this investigation, 5-ethyl-7-butyltridecane. The only variation in structure was that 5-butyl-5-ethyl-tridecane contains a quaternary carbon and the 5-ethyl-7-butyltridecane contains two tertiary carbons.

4. Conclusion and Future Research

4.1 Conclusion

The purpose of the investigation was to synthesis a H-branch alkane; 5-ethyl-7-butyltridecane. The aim was achieved by initially performing two adapted Grignard reactions; the second showed an improved yield. The 3° alcohol obtained underwent subsequent purification by column chromatography, dehydration and hydrogenation.

Throughout the investigation, between each stage, analysis of the product was carried out using FT-IR, GC-FID and GC-MS. Preliminary confirmation was given by FT-IR followed by GC-FID, if reference samples of known compounds were available. However, structural identification, particularly of the desired product was limited; a limitation overcome by the detailed, comprehensive analysis of GC-MS. The interpretation of mass spectra and the identification of characteristic ions resulting from α-cleavage at the tertiary carbons, supported by the diagnostic peaks at m/z 154 and 155 for butyl-ethylalkanes in the mass spectrum of the final product, confirmed the successful synthesis of 5-ethyl-7-butyltridecane (Kenig *et al.*, 2005, Lewis *et al.*, 2009). The synthetic approach used, was similar to and followed the investigation of T-branch alkanes by Lewis et al (2009).

Two of the H-branch alkanes, including 5-ethyl-7-butyltridecane were shown to have lower retention indices, at 1688 and 1692 Kovats, than n-heptadecane and pristane, at 1707 Kovats. The results of this investigation, challenge previous thought that

pristane was the earliest eluting C_{19} branched alkane and that the effect of branching on the elution of an alkane, is greater than originally believed.

4.2 Future Research

The potential uses of the H-branch alkane synthesised could be to advance the chromatographic understanding of aliphatic hydrocarbons in complex mixtures such as petroleum. Following this investigation, now one series of 5,7-alkyl substituted C_{19} H-branch is completed, a mixture of the H-branch alkanes should be analysed by GC-MS to support the preliminary evidence of chromatographic effects provided by this investigation. Furthermore, a mixture of all the H-branch and T-branch alkanes could be analysed to investigate certain matrix effects on the retention index to give an insight to the matrix effects occurring in more complex mixtures e.g. petroleum.

Synthesis of all the C_{19} H-branch alkanes should be undertaken to see if any other H-branch alkanes retain even lower retention indices. The overall aim of further synthesis is to advance the understanding of the aliphatic fraction of the UCM and investigate the solubility and toxicological effects within the environment.

References

Albaigés, J., Frei, R. W., Merian, E., Chemistry, I. a. O. E. A. & Societat Catalana De Ciències Físiques, Q. I. M. 1983. *Chemistry and analysis of hydrocarbons in the environment*, Gordon and Breach Science Publishers.

Belt, S. T., Allard, W. G., Rintatalo, J., Johns, L. A., Van Duin, A. C. T. & Rowland, S. J. 2000. Clay and acid catalysed isomerisation and cyclisation reactions of highly branched isoprenoid (HBI) alkenes: implications for sedimentary reactions and distributions. *Geochimica et Cosmochimica Acta,* 64**,** 3337-3345.

Boehm, P. D., Douglas, G. S., Burns, W. A., Mankiewicz, P. J., Page, D. S. & Bence, A. E. 1997. Application of petroleum hydrocarbon chemical fingerprinting and allocation techniques after the Exxon Valdez oil spill. *Marine Pollution Bulletin,* 34**,** 599-613.

Booth, A. M., Sutton, P. A., Lewis, C. A., Lewis, A. C., Scarlett, A., Chau, W., Widdows, J. & Rowland, S. J. 2006. Unresolved Complex Mixtures of Aromatic Hydrocarbons: Thousands of Overlooked Persistent, Bioaccumulative, and Toxic Contaminants in Mussels. *Environmental Science & Technology,* 41**,** 457-464.

Burns, K. A., Greenwood, P., Benner, R., Brinkman, D., Brunskill, G., Codi, S. & Zagorskis, I. 2004. Organic biomarkers for tracing carbon cycling in the Gulf of Papua (Papua New Guinea). *Continental Shelf Research,* 24**,** 2373-2394.

Canonne, P., Foscolos, G., Caron, H. & Lemay, G. 1982. Etude de l'influence du diluant hydrocarbone dans la reaction des organomagnesiens primaires sur les cetones encombrees. *Tetrahedron,* 38**,** 3563-3568.

Clayden, J., Greeves, N., Warren, S. & Wothers, P. 2001. *Organic chemistry*, Oxford University Press.

Crippen, R. C. 1973. *Identification of organic compounds with the aid of gas chromatography*, McGraw-Hill.

Dass, C. 2007. *Fundamentals of contemporary mass spectrometry*, Wiley-Interscience.

Donkin, P., Smith, E. L. & Rowland, S. J. 2003. Toxic Effects of Unresolved Complex Mixtures of Aromatic Hydrocarbons Accumulated by Mussels, Mytilus edulis, from Contaminated Field Sites. *Environmental Science & Technology,* 37**,** 4825-4830.

Engel, M. H. & Macko, S. A. 1993. *Organic geochemistry: principles and applications*, Plenum Press.

Frysinger, G. S., Gaines, R. B., Xu, L. & Reddy, C. M. 2003. Resolving the Unresolved Complex Mixture in Petroleum-Contaminated Sediments. *Environmental Science & Technology,* 37**,** 1653-1662.

Garner, C. M. 1997. *Techniques and experiments for advanced organic laboratory*, Wiley.

Gough, M. & Rowland, S. 1991. Characterization of unresolved complex mixtures of hydrocarbons from lubricating oil feedstocks. *Energy & Fuels,* 5**,** 869-874.

Gough, M. A., Rhead, M. M. & Rowland, S. J. 1992. Biodegradation studies of unresolved complex mixtures of hydrocarbons: model UCM hydrocarbons and the aliphatic UCM. *Organic Geochemistry,* 18**,** 17-22.

Gough, M. A. & Rowland, S. J. 1990. Characterization of unresolved complex mixtures of hydrocarbons in petroleum. *Nature,* 344**,** 648-650.

Gross, J. H. 2011. *Mass Spectrometry: A Textbook*, Springer.

Günzler, H. & Gremlich, H. U. 2002. *IR spectroscopy: an introduction*, Wiley-VCH.

Guidechem. 2012. *20R 23S 24R-DINOSTERANE* [Online]. Chemical Trading Guide. Available: http://www.guidechem.com/cas-146/146276-34-8.html [Accessed 25/03/12.

Headley, J. V., Barrow, M. P., Peru, K. M., Fahlman, B., Frank, R. A., Bickerton, G., Mcmaster, M. E., Parrott, J. & Hewitt, L. M. 2011. Preliminary fingerprinting of Athabasca oil sands polar organics in environmental samples using electrospray ionization Fourier transform ion cyclotron resonance mass spectrometry. *Rapid Communications in Mass Spectrometry,* 25**,** 1899-1909.

Kelly, B. 1998. *Organic II Laboratory: Grignard Reaction* [Online]. Southwestern Oklahoma State University. Available: http://faculty.swosu.edu/william.kelly/pdf/grign.pdf [Accessed 16/03/12.

Kenig, F., Simons, D.-J. H., Crich, D., Cowen, J. P., Ventura, G. T. & Rehbein-Khalily, T. 2005. Structure and distribution of branched aliphatic alkanes with

quaternary carbon atoms in Cenomanian and Turonian black shales of Pasquia Hills (Saskatchewan, Canada). *Organic Geochemistry,* 36**,** 117-138.

Kenig, F., Simons, D.-J. H., Crich, D., Cowen, J. P., Ventura, G. T., Rehbein-Khalily, T., Brown, T. C. & Anderson, K. B. 2003. Branched aliphatic alkanes with quaternary substituted carbon atoms in modern and ancient geologic samples. *Proceedings of the National Academy of Sciences,* 100**,** 12554-12558.

Kenig, F., Sinninghe Damsté, J. S., Kock-Van Dalen, A. C., Rijpstra, W. I. C., Huc, A. Y. & De Leeuw, J. W. 1995. Occurrence and origin of mono-, di-, and trimethylalkanes in modern and Holocene cyanobacterial mats from Abu Dhabi, United Arab Emirates. *Geochimica et Cosmochimica Acta,* 59**,** 2999-3015.

Killops, S. D. & Killops, V. J. 2005. *Introduction to organic geochemistry*, Blackwell Pub.

Kissin, Y. V. 1987. Catagenesis and composition of petroleum: Origin of n-alkanes and isoalkanes in petroleum crudes. *Geochimica et Cosmochimica Acta,* 51**,** 2445-2457.

Komiya, S. 1997. *Synthesis of organometallic compounds: a practical guide*, J. Wiley & Sons.

Kürti, L. & Czakó, B. 2005. *Strategic applications of named reactions in organic synthesis: background and detailed mechanisms*, Elsevier Academic Press.

Lewis, C. A. 2011. EOE2602 Laboratory Practical Script: Grignard Reagents. University of Plymouth.

Lewis, C. A., Rowland, S. J. & West, C. E. 2009. How to Get the Hump. University of Plymouth.

Mansuy, L., Philp, R. P. & Allen, J. 1997. Source Identification of Oil Spills Based on the Isotopic Composition of Individual Components in Weathered Oil Samples. *Environmental Science & Technology,* 31**,** 3417-3425.

Mao, D., Weghe, H. V. D., Lookman, R., Vanermen, G., Brucker, N. D. & Diels, L. 2009. Resolving the unresolved complex mixture in motor oils using high-performance liquid chromatography followed by comprehensive two-dimensional gas chromatography. *Fuel,* 88**,** 312-318.

Marukawa, K., Takikawa, H. & Mori, K. 2001. Synthesis of the enantiomers of some methyl-branched cuticular hydrocarbons of the ant, Diacamma sp. *Biosci., Biotechnol. Biochem.,* 65.

Mayo, D. W., Pike, R. M. & Trumper, P. K. 2000. *Microscale organic laboratory: with multistep and multiscale syntheses*, Wiley.

Mccaffery, S. J., Davis, A. & Craig, D. 2009. Distinguishing between Natural Crude Oil Seepage and Anthropogenic Petroleum Hydrocarbons in Soils at a Crude

Oil Processing Facility, Coastal California. *Environmental Forensics,* 10**,** 162-174.

Mccarthy, E. D., Han, J. & Calvin, M. 1968. Hydrogen atom transfer in mass spectrometric fragmentation patterns of saturated aliphatic hydrocarbons. *Analytical Chemistry,* 40**,** 1475-1480.

Mclafferty, F. W. & TurečEk, F. 1993. *Interpretation of mass spectra*, University Science Books.

Melbye, A. G., Brakstad, O. G., Hokstad, J. N., Gregersen, I. K., Hansen, B. H., Booth, A. M., Rowland, S. J. & Tollefsen, K. E. 2009. Chemical and toxicological characterization of an unresolved complex mixture-rich biodegraded crude oil. *Environmental Toxicology and Chemistry,* 28**,** 1815-1824.

Miles, J. A. 1989. *Illustrated glossary of petroleum geochemistry*, Clarendon Press.

Nelson, D. R. & Sukkestad, D. R. 1970. Normal and branched aliphatic hydrocarbons from the eggs of the tobacco hornworm. *Biochemistry,* 9**,** 4601-4611.

Retrosynthesis. 2012. *Organic Synthesis and Carbon-Carbon Bond Forming Reactions* [Online]. UEA. Available: http://www.uea.ac.uk/~c286/notes/retrosynthesis.htm [Accessed 21/02/2012.

Rowland, S. J., Scarlett, A. G., Jones, D., West, C. E. & Frank, R. A. 2011. Diamonds in the Rough: Identification of Individual Naphthenic Acids in Oil Sands Process Water. *Environmental Science & Technology,* 45**,** 3154-3159.

Sharma, N. P. 1998. *Dictionary Of Chemistry*, Gyan Publishing House.

Silverman, G. S. & Rakita, P. E. 1996. *Handbook of Grignard reagents*, Marcel Dekker.

Smith, E., Wraige, E., Donkin, P. & Rowland, S. 2001. Hydrocarbon humps in the marine environment: Synthesis, toxicity, and aqueous solubility of monoaromatic compounds. *Environmental Toxicology and Chemistry,* 20**,** 2428-2432.

Smith, M. & March, J. 2007. *March's advanced organic chemistry: reactions, mechanisms, and structure*, Wiley-Interscience.

Smith, M. B. 2011. *Organic Synthesis*, Elsevier Science.

Smith, R. M. 2004. *Understanding Mass Spectra: A Basic Approach*, John Wiley & Sons.

Sparkman, O. D., Penton, Z. & Kitson, F. G. 2011. *Gas Chromatography and Mass Spectrometry: A Practical Guide*, Elsevier.

Stuart, B. & Ando, D. J. 1996. *Modern infrared spectroscopy*, Published on behalf of ACOL (University of Greenwich) by Wiley.

Summons, R. E., Thomas, J., Maxwell, J. R. & Boreham, C. J. 1992. Secular and environmental constraints on the occurrence of dinosterane in sediments. *Geochimica et Cosmochimica Acta,* 56**,** 2437-2444.

Thomas, K. V., Donkin, P. & Rowland, S. J. 1995. Toxicity enhancement of an aliphatic petrogenic unresolved complex mixture (UCM) by chemical oxidation. *Water Research,* 29**,** 379-382.

Wang, Z. & Stout, S. A. 2007. *Oil spill environmental forensics: fingerprinting and source identification*, Elsevier/Academic Press.

Warton, B., Alexander, R. & Kagi, R. I. 1997. Identification of some single branched alkanes in crude oils. *Organic Geochemistry,* 27**,** 465-476.

Wauquier, J. P. 1995. *Petroleum Refining: Crude oil, petroleum products, process flowsheets*, Éditions Technip.

Webbook, N. 2012. *NIST Chemistry Webbook: NIST Standard Reference Database Number 69* [Online]. Available: http://webbook.nist.gov/chemistry/ [Accessed 17/03/12.

Wells, P. G., Butler, J. N. & Hughes, J. S. 1995. *Exxon Valdez oil spill: fate and effects in Alaskan waters*, ASTM.

Wraige, E. 1997. *Studies of the synthesis, environmental occurrence and toxicity of unresolved complex mixtures (UCMs) of hydrocarbons.* Ph.D, University of Plymouth.

Zarbin, P. H. G., Princival, J. L., De Lima, E. R., Dos Santos, A. A., Ambrogio, B. G. & De Oliveira, A. R. M. 2004. Unsymmetrical double Wittig olefination on the syntheses of insect pheromones. Part 1: Synthesis of 5,9-dimethylpentadecane, the sexual pheromone of Leucoptera coffeella. *Tetrahedron Letters,* 45**,** 239-241.